Cell Reports

Article

# Cytochrome *c* regulates hyphal morphogenesis by interfering with cAMP-PKA signaling in *Candida albicans*

## Graphical abstract

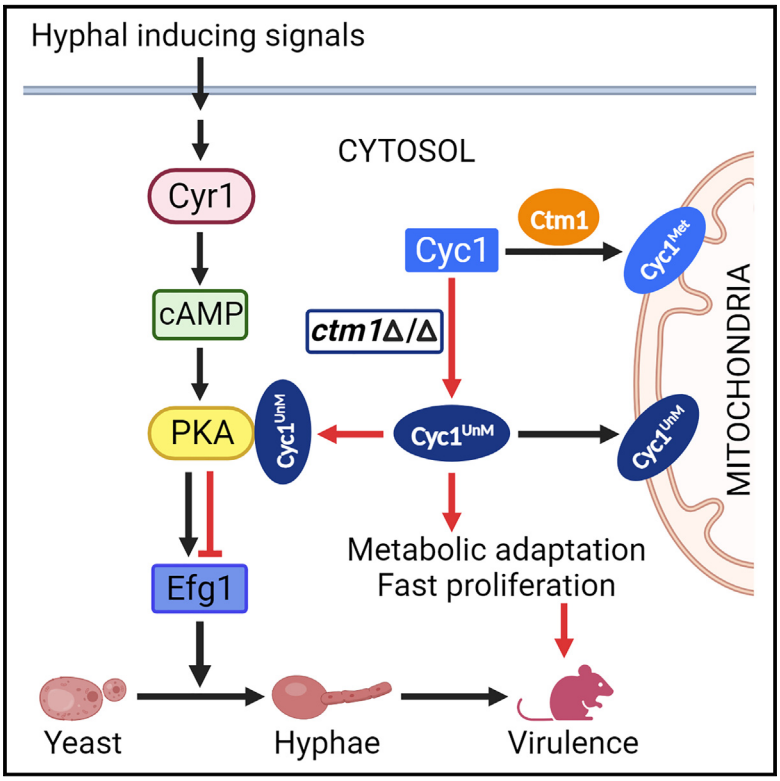


## Highlights

- The methyltransferase Ctm1 is essential for the hyphal growth of *Candida albicans*
- Ctm1 specifically catalyzes the trimethylation of cytochrome *c* (Cyc1) at lysine 79
- Unmethylated Cyc1 binds to the catalytic subunits of PKA and inhibits their kinase activity
- *ctm1*Δ/Δ mutant retains virulence in mice by improving proliferation via metabolic adaptation

## Authors

Guisheng Zeng, Xiaoli Xu, Yee Jiun Kok, ..., Jiaxin Gao, Xuezhi Bi, Yue Wang

## Correspondence

zeng_guisheng@idlabs.a-star.edu.sg (G.Z.), wang_yue@idlabs.a-star.edu.sg (Y.W.)

## In brief

Through a transposon-mediated genetic screen, Zeng et al. identify the methyltransferase Ctm1 as a critical regulator of hyphal growth. Ctm1 specifically methylates cytochrome *c* (Cyc1) at lysine 79. Unmethylated Cyc1 binds to the catalytic subunits of protein kinase A and inhibits their activity, blocking cAMP-PKA signaling and hyphal development.

Zeng et al., 2023, Cell Reports *42*, 113473
December 26, 2023 
https://doi.org/10.1016/j.celrep.2023.113473

CellPress

Cell Reports

CellPress
OPEN ACCESS

Article

# Cytochrome *c* regulates hyphal morphogenesis by interfering with cAMP-PKA signaling in *Candida albicans*

Guisheng Zeng,[1,*] Xiaoli Xu,[1] Yee Jiun Kok,[2] Fu-Sheng Deng,[3] Eve Wai Ling Chow,[1] Jiaxin Gao,[4] Xuezhi Bi,[2,5] and Yue Wang[1,6,7,*]

[1]A*STAR Infectious Diseases Labs (A*STAR ID Labs), Agency for Science, Technology and Research (A*STAR), 8A Biomedical Grove, #05-13 Immunos, Singapore 138648, Singapore
[2]Bioprocessing Technology Institute, 20 Biopolis Way, #06-01 Centros, Singapore 138668, Singapore
[3]Department of Biochemical Science and Technology, College of Life Science, National Taiwan University, Taipei 10617, Taiwan
[4]State Key Laboratory of Mycology, Institute of Microbiology, Chinese Academy of Sciences, Beijing 100101, China
[5]Duke-NUS Medical School, National University of Singapore, Singapore 169857, Singapore
[6]Department of Biochemistry, Yong Loo Lin School of Medicine, National University of Singapore, Singapore 117597, Singapore
[7]Lead contact
*Correspondence: zeng_guisheng@idlabs.a-star.edu.sg (G.Z.), wang_yue@idlabs.a-star.edu.sg (Y.W.)
https://doi.org/10.1016/j.celrep.2023.113473

## SUMMARY

In the human fungal pathogen *Candida albicans*, invasive hyphal growth is a well-recognized virulence trait. We employed transposon-mediated genome-wide mutagenesis, revealing that inactivating *CTM1* blocks hyphal growth. *CTM1* encodes a lysine (K) methyltransferase, which trimethylates cytochrome *c* (Cyc1) at K79. Mutants lacking *CTM1* or expressing *cyc1*$^{K79A}$ grow as yeast under hyphae-inducing conditions, indicating that unmethylated Cyc1 suppresses hyphal growth. Transcriptomic analyses detected increased levels of the hyphal repressor *NRG1* and decreased levels of hyphae-specific genes in *ctm1*Δ/Δ and *cyc1*$^{K79A}$ mutants, suggesting cyclic AMP (cAMP)-protein kinase A (PKA) signaling suppression. Co-immunoprecipitation and *in vitro* kinase assays demonstrated that unmethylated Cyc1 inhibits PKA kinase activity. Surprisingly, hyphae-defective *ctm1*Δ/Δ and *cyc1*$^{K79A}$ mutants remain virulent in mice due to accelerated proliferation. Our results unveil a critical role for cytochrome *c* in maintaining the virulence of *C. albicans* by orchestrating proliferation, growth mode, and metabolism. Importantly, this study identifies a biological function for lysine methylation on cytochrome *c*.

## INTRODUCTION

*Candida albicans* is an opportunistic fungal pathogen of humans.[1] While it is a member of the host microbiota on the skin and within gastrointestinal tract in healthy individuals, it is also the leading cause of systemic fungal infections in immunocompromised patients.[2,3] This problem is exacerbated by the global emergence of multi-drug-resistant *C. albicans*, posing a public health threat.[4] To combat invasive fungal infections, it is imperative to elucidate the mechanisms that govern the pathogenicity and virulence of the pathogen in order to design therapeutic strategies.

*C. albicans* is polymorphic, switching between three primary morphologies in response to environmental cues: yeast, pseudohyphae, and hyphae.[5,6] The yeast form is generally considered the commensal state, while hyphae are invasive, penetrating host tissues and escaping phagocytic cells. Hyphae express surface adhesins, facilitating attachment to host cells.[7] They also secrete hydrolytic enzymes[8] and the toxin candidalysin,[9] which damage host cells and tissues.[10] Given the crucial role of hyphae in *C. albicans* virulence, many efforts have been made to search for inhibitors of hyphal growth as an avenue to develop new antifungal drugs.[11,12]

Several signaling pathways control the hyphal growth of *C. albicans* by regulating the expression of hyphae-specific genes (HSGs).[6,13,14] Among these pathways, cyclic AMP (cAMP)-protein kinase A (PKA) signaling plays a central role.[6] A critical component of this pathway is the adenylate cyclase Cyr1, a multi-domain protein that can sense and integrate multiple signals to control cAMP production.[15] cAMP binds to the regulatory subunits of PKA, releasing its active catalytic subunits. This leads to the activation of transcription factors such as Efg1 and the downregulation of transcription repressors such as Tup1 and Nrg1. These activities promote HSG's expression, which, in turn, governs hyphal morphogenesis and other virulence-related traits.[13]

During commensalism and systemic infection, *C. albicans* encounters diverse host niches and deftly reprograms its metabolism to adapt to the local nutrient supply.[16–19] Besides being the powerhouse of eukaryotic cells, the mitochondrion plays a

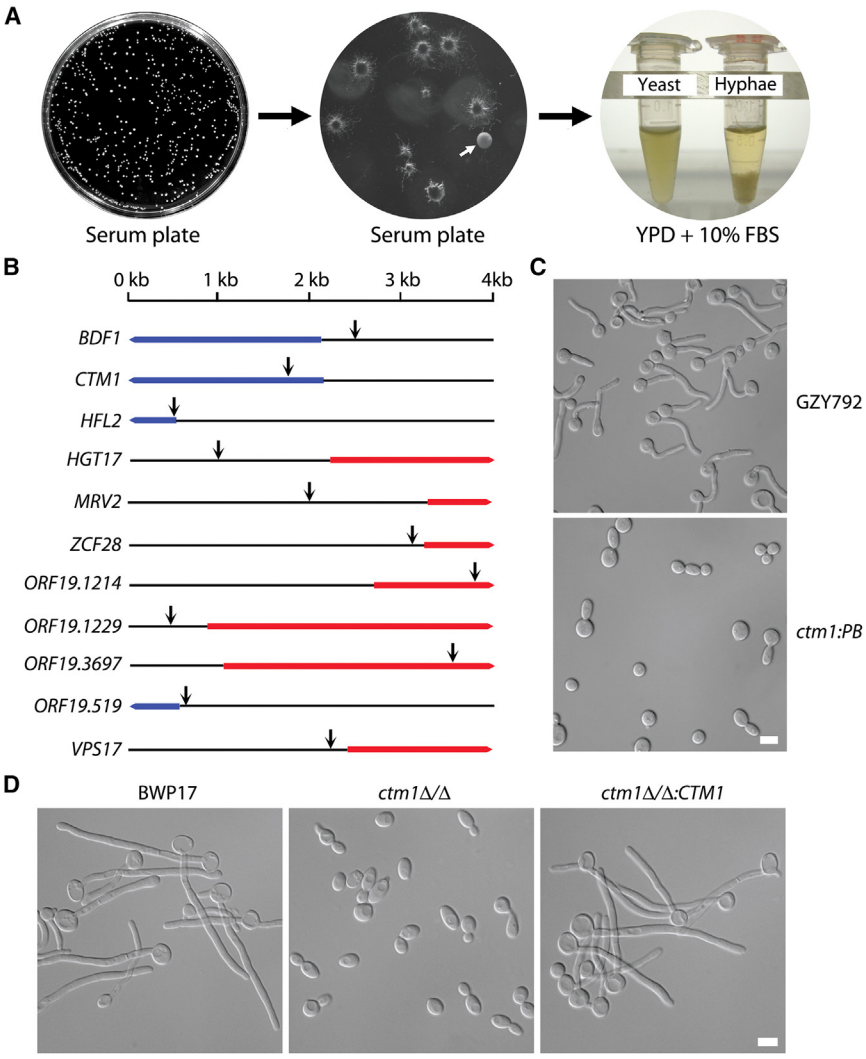


**Figure 1. Identification of *CTM1* as a novel regulator of hyphal morphogenesis in *C. albicans***

(A) Procedures of genetic screen. Haploid mutant cells were grown on serum plates at 37°C for 3 days. Colonies typical of yeast cells (arrow) were retested for hyphal growth in liquid medium.

(B) Identification of *PB* insertion site (arrow) in haploid mutants by inverse PCR and DNA sequencing. Blue indicates genes on the Crick strand and red indicates genes on the Watson strand of a chromosome.

(C and D) Defective hyphal growth of ctm1 haploid (C) and diploid (D) mutants. Haploid strains GZY792 (WT) and ctm1:PB (HIM02) and diploid strains BWP17 (WT), ctm1Δ/Δ (GZY1275), and ctm1Δ/Δ:CTM1 (GZY1277) were induced for hyphal growth with 10% FBS at 37°C for 2 h. Bars, 5 μm.

vital role in metabolism.[20] Recent findings have expanded mitochondrion's role as a signaling hub, orchestrating diverse cellular activities in coordination with metabolic state.[21] In *C. albicans*, mitochondrial activities have been linked to signaling pathways that make the yeast-hyphal decision.[22] For example, blocking mitochondrial respiration decreases the cellular level of GTP-Ras1, dampening cAMP-PKA signaling and HSG expression.[23–25] Recently, Koch et al. proposed a mitochondrial "metabolic checkpoint" concept for the yeast-to-hyphal transition.[26]

Cytochrome *c* (Cyt-C) is a mitochondrial electron transport chain (ETC) component synthesized in the cytosol and transported into the intermembrane space of mitochondria.[27] Its canonical function is transferring electrons from complex III to IV.[28] Cyt-C is also a signaling molecule, famously known for triggering apoptosis.[29,30] Cyt-C is modified by trimethylation at a specific lysine (K) residue in fungi and plants. In *Saccharomyces cerevisiae*, Cyt-C (known as Cyc1) is trimethylated at K78 by the methyltransferase Ctm1.[31] The same trimethylation of Cyt-C by a dedicated methyltransferase has been documented in many fungal and plant species.[32–35] However, blocking this modification neither affects Cyt-C's role in the ETC nor causes any observable defects in *S. cerevisiae*.[36] Thus, the biological role of this evolutionarily conserved molecular event in plants and fungi remains a mystery.

This study has identified the methyltransferase Ctm1 as a critical regulator of hyphal morphogenesis in *C. albicans*. Blocking Ctm1's trimethylation of Cyc1 at K79 inhibits hyphal morphogenesis. Unmethylated Cyc1 binds to the catalytic subunits of PKA and inhibits their kinase activity, suppressing cAMP-PKA signaling and hyphal development. Despite lacking hyphal growth, *ctm1*Δ/Δ and *cyc1*$^{K79A}$ mutants remain virulent in a mouse model of systemic infection, likely due to increased proliferation rate. The mutants also exhibited faster growth than the wild-type (WT) strain in media supplemented with physiologically relevant nutrients. The results suggest that *C. albicans* can accelerate proliferation to compensate for the loss of hyphal development via metabolic reprogramming to maintain virulence. Additionally, we discover a biological function for the mysterious cytochrome *c* trimethylation.

## RESULTS

### *CTM1* is a regulator of *C. albicans* hyphal growth

We used *piggyBac* (*PB*) transposon-mediated mutagenesis to generate a mutant library in haploid *C. albicans*.[37] About 60,000 mutant cells were spread onto agar plates containing 10% fetal bovine serum (FBS) to a density allowing the formation of well-isolated colonies (Figure 1A) and incubated at 37°C for 3 days. While most colonies produced long filaments, some failed to do so (Figure 1A), suggesting defective hyphal growth. Altogether, 423 such colonies were picked for further

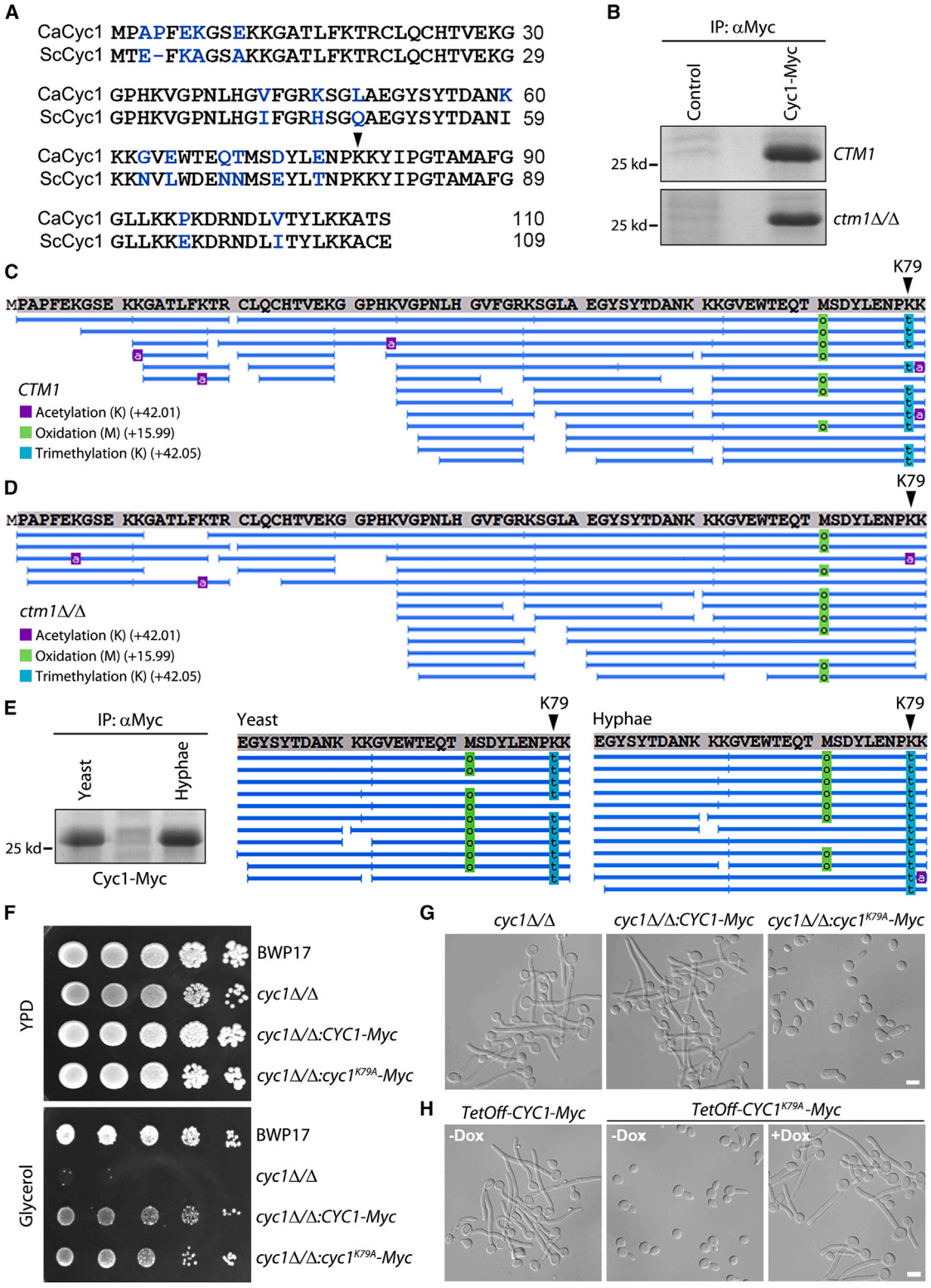


**Figure 2. Ctm1 trimethylates Cyc1 on K79 and unmethylated Cyc1 inhibits hyphal growth**

(A) Alignment of CaCyc1 and ScCyc1. Non-conserved residues are colored in blue. The arrowhead indicates the lysine (K) residue trimethylated by Ctm1 in *S. cerevisiae*.

*(legend continued on next page)*

examination of hyphal growth in liquid medium (Figure 1A), revealing 29 colonies that displayed varying degrees of hyphal defects (Figure S1).

We mapped the *PB* insertion site in each mutant by inverse PCR and DNA sequencing as previously described.[37] We identified 16 genes (Table S3) with a *PB* insertion within the coding sequence or the promoter region (Figure 1B). These genes included several known hyphal regulators, and the rest have not been implicated in hyphal morphogenesis (Table S3).

One of the identified genes, *CTM1*, encodes a putative lysine methyltransferase. The *ctm1:PB* mutant grew exclusively as yeast under hyphal-inducing conditions (Figure 1C). The *ctm1*Δ/Δ mutant constructed in the diploid strain BWP17 exhibited the same hyphal defect (Figure 1D). Reintroducing a WT copy of *CTM1* into the mutant (*ctm1*Δ/Δ*:CTM1*) restored hyphal growth (Figure 1D). These results demonstrate that *CTM1* is required for hyphal morphogenesis in *C. albicans*.

## Ctm1 specifically trimethylates Cyc1 at K79 in *C. albicans*

The Ctm1 ortholog in *S. cerevisiae* trimethylates *S. cerevisiae* Cyc1 (ScCyc1) at K78.[31] The amino acid sequences of *C. albicans* Cyc1 (CaCyc1) and ScCyc1 are nearly identical, with K79 of CaCyc1 corresponding to K78 of ScCyc1 (Figure 2A). To determine whether Ctm1 methylates Cyc1 at K79 in *C. albicans*, we tagged Cyc1 with a C-terminal Myc in WT and *ctm1*Δ/Δ strains and immunopurified Cyc1-Myc from the resulting strains (Figure 2B) for mass spectrometry (MS) analysis. We identified trimethylation of Cyc1 specifically at K79 only in WT (Figure 2C) but not in *ctm1*Δ/Δ (Figure 2D), confirming that Ctm1 trimethylates K79 of Cyc1 in *C. albicans*, indicating an evolutionarily conserved function.

Intriguingly, we found that Cyc1 from WT was primarily in the methylated form in both yeast and hyphal growth conditions (Figure 2E). However, the MS analysis was not sufficiently quantitative to accurately compare the relative levels of Cyc1 trimethylation between yeast and hyphae (see below).

## Unmethylated Cyc1 inhibits hyphal growth

The deletion of *CTM1* blocked both hyphal growth (Figure 1D) and Cyc1 trimethylation (Figure 2D), suggesting that Ctm1 might regulate hyphal morphogenesis via controlling Cyc1 methylation. To investigate this possibility, we constructed a *cyc1*Δ/Δ mutant expressing the *cyc1*$^{K79A}$ allele (*cyc1*Δ/Δ*:cyc1*$^{K79A}$) from the native promoter, replacing K79 with alanine to block methylation. Cyc1 is essential for electron transport[38] and required for survival when a nonfermentable substrate, such as glycerol, is the sole carbon source.[39] Consistently, *cyc1*Δ/Δ failed to grow on the medium with glycerol as the sole carbon source while it grew well on YPD plates, albeit slightly slower than WT (Figure 2F). The growth defect on glycerol plates was rescued by reintroducing a copy of WT *CYC1* or, more interestingly, *cyc1*$^{K79A}$ (Figure 2F), suggesting that Cyc1$^{K79A}$ is functional in electron transfer.

Surprisingly, *cyc1*Δ/Δ exhibited hyphal growth like the control (*cyc1*Δ/Δ*:CYC1*) under inducing conditions, indicating that Cyc1 is not required for hyphal development. In contrast, most *cyc1*Δ/Δ*:cyc1*$^{K79A}$ grew as yeast, with some cells having an elongated bud (Figure 2G). As Cyc1$^{K79A}$ is the only form of Cyt-C in *cyc1*Δ/Δ*:cyc1*$^{K79A}$, the result suggests that unmethylated Cyc1 (referred to as Cyc1$^{UnM}$ hereafter, which includes Cyc1$^{K79A}$ and Cyc1 in *ctm1*Δ/Δ cells) might repress hyphal growth. We investigated this possibility by overexpressing one copy of *CYC1* or *cyc1*$^{K79A}$ from the *TetOff* promoter in WT. Figure 2H shows that *CYC1*-expressing cells (−Dox) grew long hyphae upon serum induction, while *cyc1*$^{K79A}$-expressing cells (−Dox) did not, indicating that Cyc1$^{K79A}$ dominates WT Cyc1 in repressing hyphal morphogenesis. Moreover, shutting down *cyc1*$^{K79A}$ expression (+Dox) restored hyphal growth. These results suggest that Cyc1$^{UnM}$ is a hyphal repressor while retaining its electron transport function.

## Cyc1$^{UnM}$ downregulates HSGs and upregulates *NRG1*

To understand how Cyc1$^{UnM}$ inhibits hyphal growth, we performed RNA sequencing (RNA-seq) analysis, comparing WT (BWP17), *ctm1*Δ/Δ, and *cyc1*$^{K79A}$ cells grown in yeast and hyphal-inducing conditions (Table S4). We took three types of samples: overnight yeast cultures and 1-h or 2-h hyphal-inducing cultures (Figure 3A). With a $\log_2$ fold change (logFC) of 0.5 as the cutoff value and both false discovery rate (FDR) and p value smaller than 0.05, upregulation of many HSGs, such as *ALS3*, *ECE1*, *HWP1*, and *UME6*, and downregulation of three hyphal suppressor genes (*TUP1*, *NRG1*, and *RFG1*) were observed in WT at hyphae-1h and hyphae-2h (Figure 3B), indicating successful hyphal induction. Intriguingly, we found similar up- and downregulation of HSGs and hyphal repressor genes in *ctm1*Δ/Δ and *cyc1*$^{K79A}$ upon hyphal induction (Figures 3C and 3D), despite most mutant cells remaining as yeast throughout the induction.

To elucidate why the upregulation of HSGs and downregulation of hyphal suppressors in *ctm1*Δ/Δ and *cyc1*$^{K79A}$ did not result in hyphal growth, we defined the gene transcript level in cells cultured in the yeast growth condition as the basal level

(B) Immunoprecipitation of Cyc1-Myc for MS analysis. Cyc1-Myc was immunoprecipitated from GZY1313 (*CTM1:CYC1-Myc*) and GZY1348 (*ctm1*Δ/Δ*:CYC1-Myc*) cell extracts, separated by SDS-PAGE, and stained. The protein band was then excised for MS analysis.
(C and D) Results of MS analysis of Cyc1-Myc purified from WT (*CTM1*) and *ctm1*Δ/Δ cells.
(E) MS analysis of Cyc1 methylation in yeast and hyphal cells. GZY1313 cells were cultured in Yeast Extract Peptone Dextrose (YPD) at 30°C (yeast) or further induced with 10% FBS at 37°C for 2 h (hyphae). Cyc1-Myc was immunopurified from both samples for MS analysis. Arrowheads indicate K79.
(F) Cyc1$^{K79A}$ is functional in ETC. Cultures of BWP17, *cyc1*Δ/Δ (GZY1300), *cyc1*Δ/Δ*:CYC1-Myc* (GZY1313), and *cyc1*Δ/Δ*:cyc1*$^{K79A}$*-Myc* (GZY1314) were adjusted to optical density 600 ($OD_{600}$) = 1 and serially diluted by 10-fold. Then 5 μL of each dilution was spotted onto YPD and glycerol minimal-medium plates and incubated at 30°C for 2 and 7 days, respectively.
(G) Defective hyphal growth of the *cyc1*Δ/Δ*:cyc1*$^{K79A}$ mutant. BWP17, *cyc1*Δ/Δ*:CYC1-Myc*, and *cyc1*Δ/Δ*:cyc1*$^{K79A}$*-Myc* were induced for hyphal growth in YPD containing 10% FBS at 37°C for 2 h.
(H) *CYC1*$^{K79A}$ overexpression inhibits serum-induced hyphal growth. BWP17 overexpressing either *CYC1-Myc* (GZY1326) or *CYC1*$^{K79A}$*-Myc* (GZY1322) from the *TetOff* promoter were induced for hyphal growth (YPD with 5% FBS at 37°C for 2 h) in the presence or absence of 50 μg/mL doxycycline (Dox). Bars, 5 μm.

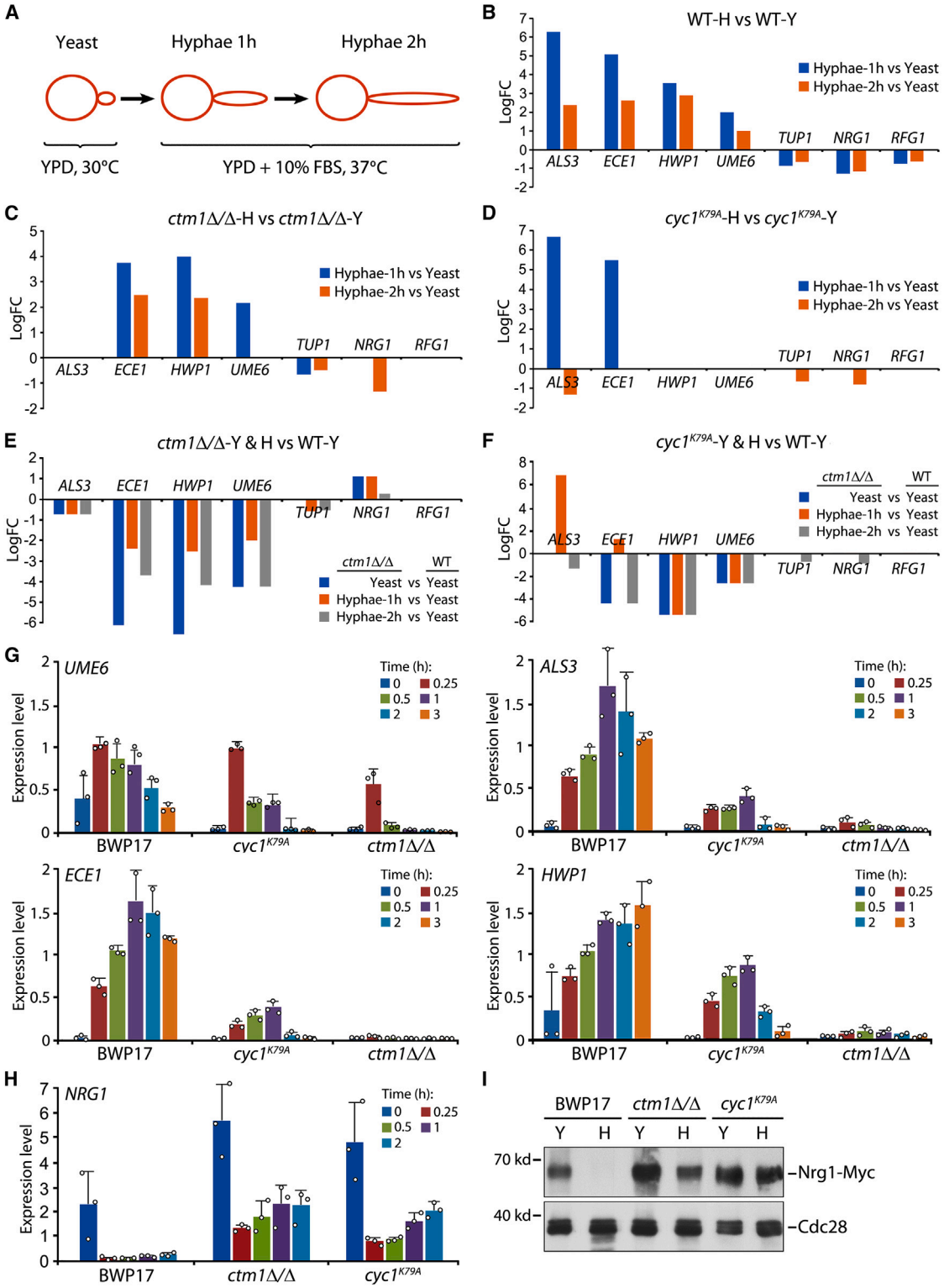


**Figure 3. *ctm1*Δ/Δ and *cyc1*$^{K79A}$ downregulate HSGs and upregulate *NRG1***

(A) Experimental procedure for RNA-seq analysis. WT (BWP17), *ctm1*Δ/Δ (GZY1275), and *cyc1*$^{K79A}$ (GZY1314) were cultured in YPD at 30°C and induced with 10% FBS for hyphal growth at 37°C for 1 and 2 h. Samples were taken at the time points indicated.

(B–D) Transcriptional changes of selected genes in WT (B), *ctm1*Δ/Δ (C), and *cyc1*$^{K79A}$ (D) cells during yeast growth and hyphal induction.

*(legend continued on next page)*

and compared it with the expression of these genes between mutants and WT. We found that the basal transcript level of *ALS3*, *ECE1*, *HWP1*, and *UME6* was 0.6, 6, 6.2, and 4.2-logfold lower in *ctm1*Δ/Δ than in WT, respectively (Figure 3E). A similar trend also occurred in *cyc1*$^{K79A}$ except for *ALS3* (Figure 3F). In contrast, the basal transcript level of *NRG1* was 1.2-logfold higher in *ctm1*Δ/Δ than in WT (Figure 3E). The basal transcript level of the three suppressor genes did not differ significantly between *cyc1*$^{K79A}$ and WT (Figure 3F). Upon hyphal induction, although the transcript levels of HSGs in *ctm1*Δ/Δ and *cyc1*$^{K79A}$ increased, they remained lower than their corresponding basal level in WT (Figures 3E and 3F). Additionally, the transcript level of *NRG1* in *ctm1*Δ/Δ remained high following the shift to hyphal growth, while that of *TUP1* and *RFG1* was comparable between the mutants and WT (Figures 3E and 3F).

We verified the RNA-seq data by measuring the transcript levels of *UME6*, *ALS3*, *ECE1*, *HWP1*, and *NRG1* by qRT-PCR during hyphal induction (Table S5). We observed varying degrees of upregulation of all four HSGs in *ctm1*Δ/Δ and *cyc1*$^{K79A}$. However, their expression levels remained markedly lower in both mutants than in WT (Figure 3G). The repression of HSG upregulation was more pronounced in *ctm1*Δ/Δ than in *cyc1*$^{K79A}$, implying that additional factor(s) may exist and function in parallel with Cyc1$^{UnM}$ to suppress hyphal growth in the *ctm1*Δ/Δ mutant. This hypothesis is supported by observations of other weaker phenotypes exhibited by the *cyc1*$^{K79A}$ mutant than the *ctm1*Δ/Δ mutant, as shown below.

Nrg1 is a repressor of HSG expression, and its deletion causes constitutive filamentation.[40,41] In WT cells, the *NRG1* transcript level dropped by >95% at 15 min of hyphal induction and remained at this low level for at least 2 h (Figure 3H). Surprisingly, the *NRG1* transcript level was approximately two times higher in *ctm1*Δ/Δ and *cyc1*$^{K79A}$ than in WT during yeast growth. Additionally, despite the decrease of *NRG1* transcript level in both mutants at 15 min of induction, it remained several folds higher compared to that in WT. Also, *NRG1* transcript levels gradually increased from 30 to 120 min of hyphal induction (Figure 3H). Consistent with previous reports,[42] we also found that the Nrg1 protein level was barely detectable in WT at 30 min of hyphal induction. In sharp contrast, Nrg1 remained at high levels in both *ctm1*Δ/Δ and *cyc1*$^{K79A}$ cells (Figure 3I).

Our data demonstrate that the basal transcript levels of HSGs in *ctm1*Δ/Δ and *cyc1*$^{K79A}$ mutants are markedly downregulated during yeast growth and do not reach the threshold required for hyphal growth, despite the hyphal-induced upregulation. Simultaneously, the levels of the hyphal repressor *NRG1* are substantially higher in the mutants than in WT during yeast growth and remain high despite the hyphal-induced downregulation. Therefore, the downregulation of HSGs and upregulation of *NRG1* in the mutants can account for the failure of *ctm1*Δ/Δ and *cyc1*$^{K79A}$ in hyphal morphogenesis.

## Cyc1$^{UnM}$ acts between cAMP and Efg1 along the cAMP-PKA pathway

The qRT-PCR data above demonstrated the upregulation of *NRG1* and downregulation of *UME6* in *ctm1*Δ/Δ and *cyc1*$^{K79A}$, suggesting that Cyc1$^{UnM}$ functions upstream of Nrg1 and Ume6. Supporting this notion, the hyphal defects of *ctm1*Δ/Δ were largely corrected by deleting *NRG1* or overexpressing *UME6*. In contrast, both *ctm1*Δ/Δ *nrg1*Δ/Δ and *ctm1*Δ/Δ*:TetOff-UME6* (−Dox) mutants grew primarily as filaments even without serum induction (Figures 4A and 4B).

In the cAMP-PKA pathway, PKA activates Efg1 by phosphorylating it at T206,[43] which, in turn, activates HSGs and represses *NRG1*.[44] The phosphomimetic mutant *efg1*$^{T206E}$ causes constitutive filamentation.[43] We found that expressing Efg1$^{T206E}$ suppressed the hyphal defects of both *ctm1*Δ/Δ and *cyc1*$^{K79A}$ and promoted filamentation under non-inducing conditions, producing filaments morphologically indistinguishable from those of *efg1*$^{T206E}$ (Figure 4C). The data indicate that Efg1 acts downstream of Cyc1$^{UnM}$.

cAMP directly activates PKA by binding to Bcy1, the regulatory subunit of PKA, to release the catalytic subunits.[45] In *C. albicans*, cAMP is synthesized by the adenylyl cyclase Cyr1, and the *cyr1*Δ/Δ mutant cannot switch to hyphal growth under nearly all inducing conditions.[46] However, addition of exogenous cAMP to the growth medium suppressed the hyphal defect of *cyr1*Δ/Δ[46] (Figure 4D). In contrast, addition of the same amount of exogenous cAMP did not restore hyphal growth to either *ctm1*Δ/Δ or *cyc1*$^{K79A}$ (Figure 4D), indicating that Cyc1$^{UnM}$ acts downstream of cAMP.

PKA is the sole component immediately downstream of cAMP and upstream of Efg1 in the cAMP-PKA pathway. Our analyses above suggest that Cyc1$^{UnM}$ may directly interact with PKA to exert its regulatory function.

## Cyc1 has both cytoplasmic and mitochondrial localization

PKA, which has two catalytic subunits, Tpk1 and Tpk2, in *C. albicans*, predominantly localizes in the nucleus and translocates to the cytoplasm upon activation by cAMP.[47,48] For Cyc1 to interact with PKA, it must localize to either the cytoplasm or the nucleus in addition to its default mitochondrial localization. Interestingly, GFP-tagged Cyc1 has been reported to exhibit both cytoplasmic and mitochondrial localization in *S. cerevisiae*.[49,50] We also tagged Cyc1 and Cyc1$^{K79A}$ with GFP in *C. albicans*. Both GFP-tagged proteins supported the growth of *cyc1*Δ/Δ on plates with glycerol as the sole

(E and F) Comparison of the transcript levels of selected genes in *ctm1*Δ/Δ (E) and *cyc1*$^{K79A}$ (F) cultured in yeast and hyphal growth conditions to those in WT cultured in yeast growth condition.

(G and H) Downregulation of *UME6*, *ASL3*, *ECE1*, and *HWP1* (G) and upregulation of *NRG1* (H) in *cyc1*$^{K79A}$ and *ctm1*Δ/Δ. BWP17, *cyc1*$^{K79A}$, and *ctm1*Δ/Δ cultures were induced with 10% FBS for hyphal growth at 37°C. Aliquots were collected at the indicated time points for qRT-PCR analysis. Data shown are the average of three independent experiments with standard deviations (SDs).

(I) Upregulation of Nrg1 protein level in *ctm1*Δ/Δ and *cyc1*$^{K79A}$. BWP17, *ctm1*Δ/Δ, and *cyc1*$^{K79A}$ expressing Nrg1-Myc (GZY1045, GZY1347, and GZY1350, respectively) were cultured in YPD at 30°C and induced for hyphal growth with 10% FBS at 37°C for 30 min. Samples were taken for protein extraction and subjected to WB using αMyc and PSTAIRE antibodies.

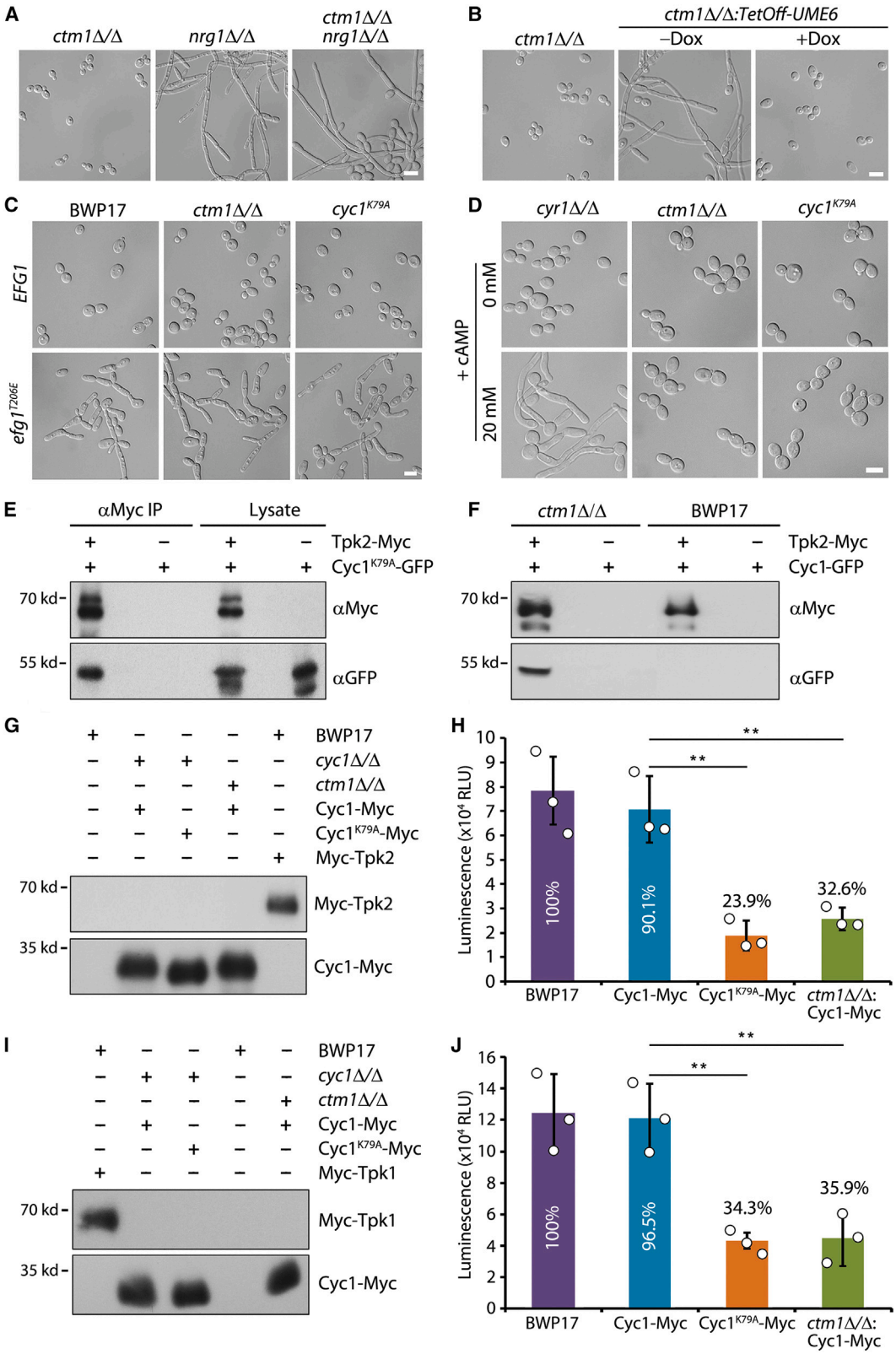


*(legend on next page)*

carbon source (Figure S2A). Upon hyphal induction, *cyc1*Δ/Δ:*CYC1-GFP* produced normal hyphae like WT while *cyc1*Δ/Δ:*CYC1*$^{K79A}$*-GFP* grew as yeast (Figure S2B). These results indicate that the GFP-tagged Cyc1 and Cyc1$^{K79A}$ are functional. Fluorescence microscopy revealed similar subcellular localization patterns for Cyc1-GFP in both *cyc1*Δ/Δ *CTM1* and *cyc1*Δ/Δ *ctm1*Δ/Δ cells, as well as Cyc1$^{K79A}$-GFP in *cyc1*-Δ/Δ cells. While some GFP signals colocalized with MitoTracker in the mitochondria, significant signals were also evident in the cytoplasm (Figure S2C).

To further confirm the cytoplasmic localization of Cyc1, we separated mitochondria from the cytosol by differential fractionation and examined the presence of Cyc1 in both fractions. We detected both methylated Cyc1 (in WT cells) and unmethylated Cyc1 (in *ctm1*Δ/Δ cells) in mitochondrial and cytoplasmic fractions by western blotting (WB). In contrast, the mitochondrion-specific protein Por1[51] was exclusively detected in the mitochondrial fraction (Figure S2D). Collectively, these data demonstrate that a fraction of Cyt-C in *C. albicans* is present in the cytoplasm aside from its localization in the mitochondria.

## Cyc1$^{UnM}$ binds to PKA and inhibits its kinase activity

Next, we performed co-immunoprecipitation (coIP) to detect association between Cyc1 and PKA. We tagged Cyc1$^{K79A}$ with GFP and Tpk2 with Myc and verified their expression by WB (Figure 4E). When Tpk2-Myc was immunoprecipitated using αMyc beads, Cyc1$^{K79A}$-GFP was detected in the immunoprecipitation (IP) products by αGFP WB (Figure 4E). We then tagged Cyc1 with GFP and Tpk2 with Myc in both WT and *ctm1*Δ/Δ to repeat the coIP. The results showed that Cyc1-GFP could be co-immunoprecipitated only in *ctm1*Δ/Δ but not in WT (Figure 4F). These results indicate that only Cyc1$^{UnM}$ physically associates with Tpk2.

To test whether Cyc1$^{UnM}$ regulates PKA activity, we immunopurified Myc-tagged Tpk2, Cyc1, and Cyc1$^{K79A}$. Aliquots of the eluted products were analyzed by αMyc WB for verification and quantification (Figure 4G). Equal amounts of Myc-Tpk2 were first incubated with 10 times more elution products from BWP17 (control for non-specific protein association with IP beads), *cyc1*Δ/Δ:Cyc1-Myc, *cyc1*Δ/Δ:Cyc1$^{K79A}$-Myc, and *ctm1*Δ/Δ:Cyc1-Myc cells, respectively, at room temperature (RT) for 30 min, followed by *in vitro* kinase assays. Compared with the control, methylated Cyc1 (from *cyc1*Δ/Δ:Cyc1-Myc) slightly reduced Tpk2 kinase activity to 90.1%. In contrast, Cyc1$^{K79A}$ (from *cyc1*Δ/Δ:Cyc1$^{K79A}$-Myc) and unmethylated Cyc1 (from *ctm1*Δ/Δ:Cyc1-Myc) suppressed Tpk2 kinase activity to 23.9% and 32.6%, respectively (Figure 4H). We further immunopurified Myc-Tpk1 (Figure 4I) to repeat the kinase assays and obtained similar results. In contrast, both Cyc1$^{K79A}$ and unmethylated Cyc1 reduced Tpk1 kinase activity to ∼35% (Figure 4J). Together, our results demonstrate that Cyc1$^{UnM}$ inhibits PKA kinase activity through a direct interaction with the catalytic subunits of PKA.

## Methylation of Cyc1 is regulatable and correlates with filamentation

We hypothesized that modulating Cyc1 methylation might be a mechanism for *C. albicans* to regulate hyphal growth under certain conditions. We used a trimethylated-lysine-specific antibody (αtmeK) to assess Cyc1's methylation level in *C. albicans*. αtmeK can readily detect Cyc1-Myc only when it was immunoprecipitated from Ctm1-expressing cells but not from *ctm1*Δ/Δ. In addition, αtmeK could not detect Cyc1$^{K79A}$, demonstrating that αtmeK specifically detects Ctm1-dependent trimethylation at K79 of Cyc1 (Figure 5A).

By using αtmeK, we detected ∼36% increase of methylated Cyc1 in hyphae compared to yeast cells, demonstrating that Cyc1 methylation level in hyphae is higher than in yeast cells (Figure 5B). Furthermore, we found that Cyc1 methylation level was elevated in cells cultured in the N-acetylglucosamine (GlcNAc) medium (Figure 5C). In contrast, Cyc1 methylation level was reduced to about 80% when cells were cultured in yeast carbon base (YCB)-BSA at 30°C and to ∼60% at 37°C (Figure 5D). Correspondingly, *C. albicans* displayed filamentation in the GlcNAc medium but grew as yeast in YCB-BSA (Figure 5E).

**Figure 4. Cyc1$^{UnM}$ interacts with PKA to inhibit the kinase activity**

(A) *nrg1*Δ/Δ causes constitutive filamentous growth in *ctm1*Δ/Δ. *ctm1*Δ/Δ (GZY1275), *ctm1*Δ/Δ *nrg1*Δ/Δ (GZY1310), and *nrg1*Δ/Δ (GZY1309) mutants were grown in YPD at 30°C.

(B) *UME6* overexpression causes filamentous growth of *ctm1*Δ/Δ. *ctm1*Δ/Δ and *ctm1*Δ/Δ*:TetOff-UME6* (GZY1319) were grown in YPD at 30°C in the presence or absence of Dox (50 μg/mL).

(C) Expression of Efg1$^{T206E}$ causes filamentous growth of *ctm1*Δ/Δ and *cyc1*$^{K79A}$. BWP17, *ctm1*Δ/Δ, *cyc1*$^{K79A}$, *efg1*$^{T206E}$ (GZY1370), *ctm1*Δ/Δ *efg1*$^{T206E}$ (GZY1372), and *cyc1*$^{K79A}$ *efg1*$^{T206E}$ (GZY1371) were cultured in YPD at 30°C.

(D) Exogenous cAMP fails to restore hyphal growth to *ctm1*Δ/Δ and *cyc1*$^{K79A}$. Both mutants were induced for hyphal growth with 10% FBS at 37°C for 2 h in the absence or presence of 20 mM exogenous cAMP. *cyr1*Δ/Δ (GZY942) was used as the control. Bars, 5 μm.

(E) Pull-down of Cyc1$^{K79A}$-GFP by Tpk2-Myc. Strains expressing Cyc1$^{K79A}$-GFP (GZY1324) or both Cyc1$^{K79A}$-GFP and Tpk2-Myc (GZY1403) were cultured for protein extraction, subjected to IP using αMyc antibody, and followed by WB with both αGFP and αMyc antibodies. The lysates were also used in WB to verify the expression of tagged proteins.

(F) Pull-down of Cyc1-GFP by Tpk2-Myc in *ctm1*Δ/Δ but not BWP17. BWP17 expressing Cyc1-GFP (GZY1447) or both Cyc1-GFP and Tpk2-Myc (GZY1448), and *ctm1*Δ/Δ expressing Cyc1-GFP (GZY1444) or both Cyc1-GFP and Tpk2-Myc (GZY1445) were used for coIP.

(G and I) Purification of Cyc1-Myc, Cyc1$^{K79A}$-Myc, Tpk2-Myc, and Tpk1-Myc. BWP17, *cyc1*Δ/Δ:Cyc1-Myc (GZY1313), *cyc1*Δ/Δ:Cyc1$^{K79A}$-Myc (GZY1314), *ctm1*Δ/Δ:Cyc1-Myc (GZY1348), BWP17:TetOff-Myc-Tpk2 (GZY1393), and BWP17:TetOff-Myc-Tpk1 (GZY1468) were cultured for protein extraction followed by IP with αMyc antibody, and the IP products were eluted with Myc peptides. Aliquots of eluted proteins were examined by WB.

(H and J) Cyc1$^{UnM}$ inhibits the kinase activity of PKA. Immunopurified Myc-Tpk2 (G) or Myc-Tpk1 (I) was pre-incubated with the elutes from BWP17, *cyc1*Δ/Δ:Cyc1-Myc, *cyc1*Δ/Δ:Cyc1$^{K79A}$-Myc, and *ctm1*Δ/Δ:Cyc1-Myc at RT for 30 min, respectively, and followed by *in vitro* kinase assays. Kinase activity was measured and quantified as relative light units (RLU). Data are presented as mean ± SD from three independent assays. The two-tailed Student's t test was used to check statistical significances and p values are indicated by asterisks (**$p \leq 0.01$). The relative kinase activities of PKA pre-incubated with other elutes against that of PKA pre-incubated with the elute from BWP17 are shown as percentages.

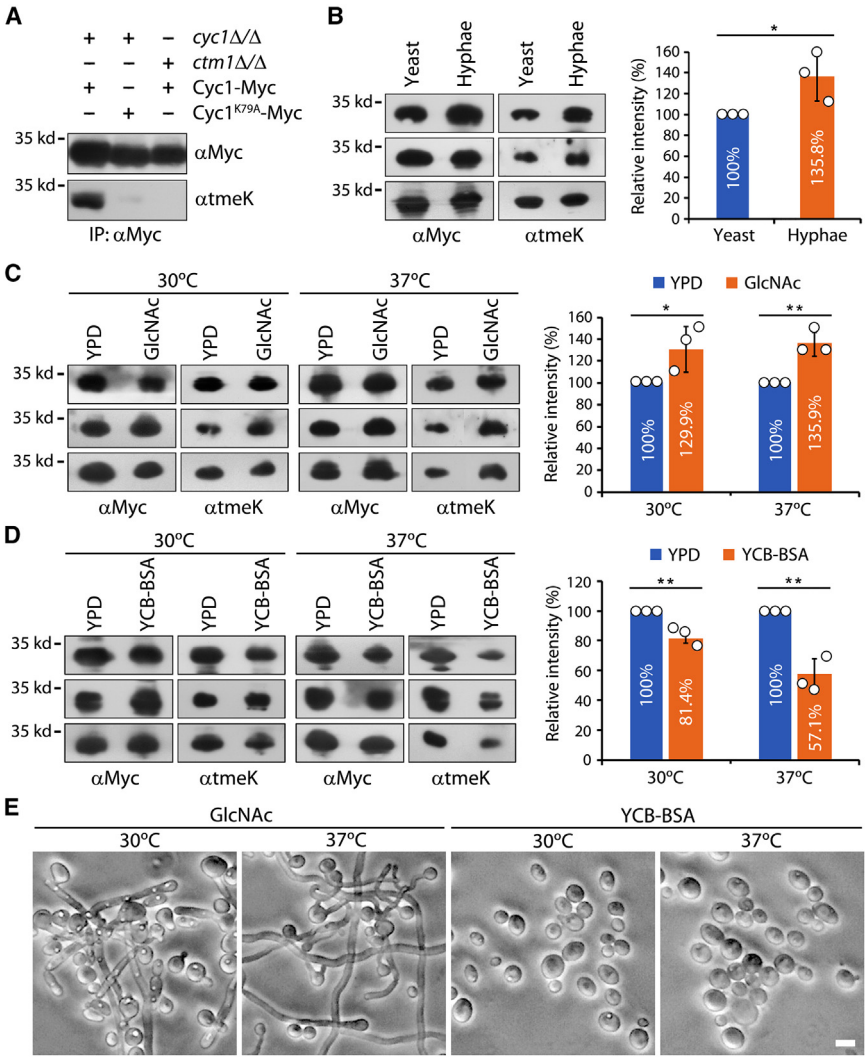


**Figure 5. Methylation of Cyc1 is regulatable and correlates with the extent of filamentation**

(A) Detection of Ctm1-dependent methylation on Cyc1. Cyc1-Myc from *cyc1*Δ/Δ (GZY1313), *ctm1*Δ/Δ (GZY1348), and Cyc1$^{K79A}$-Myc from *cyc1*Δ/Δ (GZY1314) were immunoprecipitated and sequentially probed with αtmeK and αMyc antibodies.

(B) Higher Cyc1 methylation level in yeast than in hyphal cells. GZY1313 cells were cultured in YPD at 30°C and induced for hyphal growth with 10% FBS at 37°C for 2 h.

(C) Higher Cyc1 methylation level in cells grown in GlcNAc than in YPD. GZY1313 cells were cultured in YPD or GlcNAc medium at 30°C and 37°C overnight.

(D) Lower Cyc1 methylation level in cells grown in YCB-BSA than in YPD. GZY1313 cells were cultured in YPD or YCB-BSA medium at 30°C and 37°C overnight. In (B)–(D), samples from each of the cultures were taken for protein extraction, followed by IP with αMyc antibody and WB analysis with αtmeK and αMyc antibodies. The density of a protein band (measured by ImageJ) detected with αtmeK was normalized against the density of the same protein band detected with αMyc to represent the relative methylation level. For comparison, the methylation levels of Cyc1 in hyphae against yeast (B) and in different media against YPD (C and D) were calculated and plotted. Graphs show the mean ± SD of three independent biological replicates. The one-tailed student's t test was used to check statistical significances and p values are indicated by asterisks (*$p \leq 0.05$, **$p \leq 0.01$).

(E) Morphological examination of cells culturing in GlcNAc and YCB-BSA media. GZY1313 cells were inoculated into the two media and cultured at 30°C and 37°C overnight. Bar, 5 μm.

These results demonstrate that growth conditions, such as carbon sources, serum, and temperature, can influence Cyc1's methylation level, which appears to correlate with growth modes, with low methylation levels corresponding with yeast growth and high methylation levels with hyphal growth.

### *ctm1*Δ/Δ and *cyc1*$^{K79A}$ remain virulent via accelerated yeast proliferation

We assessed the virulence of *ctm1*Δ/Δ and *cyc1*$^{K79A}$ using the mouse systemic infection model. BWP17UH, which was generated by integrating *URA3* and *HIS1* into BWP17 to ensure the same genetic background as the two mutants, was used as the WT control. For each strain, 12 mice were injected with $8 \times 10^5$ yeast cells each via the tail vein. Four mice were sacrificed at 48 h for kidney fungal burden analysis and histological examination, while the rest were monitored for survival up to 15 days. All mice infected with WT died between day 2 and 5. Surprisingly, despite the lack of hyphal growth, *ctm1*Δ/Δ and *cyc1*$^{K79A}$ also killed all mice between day 3 and 8, indicating that the mutants remained highly virulent (Figure 6A).

Kidney fungal burden analysis produced a striking result. *ctm1*Δ/Δ and *cyc1*$^{K79A}$ yielded colony-forming units (CFU) approximately 73- and 46-fold higher than WT (Figure 6B), indicating a markedly higher proliferation rate of the mutants in the kidney. Histological examination showed that kidneys infected with the mutants, especially *ctm1*Δ/Δ, contained many large, dense clusters of yeast cells (Figure 6C). In comparison, kidneys infected with WT were populated with extremely long filaments. WT hyphae are multicellular and often form clumps, leading to a significant underestimation of CFUs. Therefore, we repeated the mouse experiments and measured the fungal burden in kidney by qPCR.[52] Similar to the direct CFU counting, the qPCR method demonstrated 19- and 5-fold higher fungal burdens in mice infected with *ctm1*Δ/Δ and *cyc1*$^{K79A}$, respectively, than in those infected with WT (Figure S3). Higher fungal burdens were also observed in the brain, liver, and spleen in mice infected with *ctm1*Δ/Δ or *cyc1*$^{K79A}$ than in mice infected with WT (Figure S4).

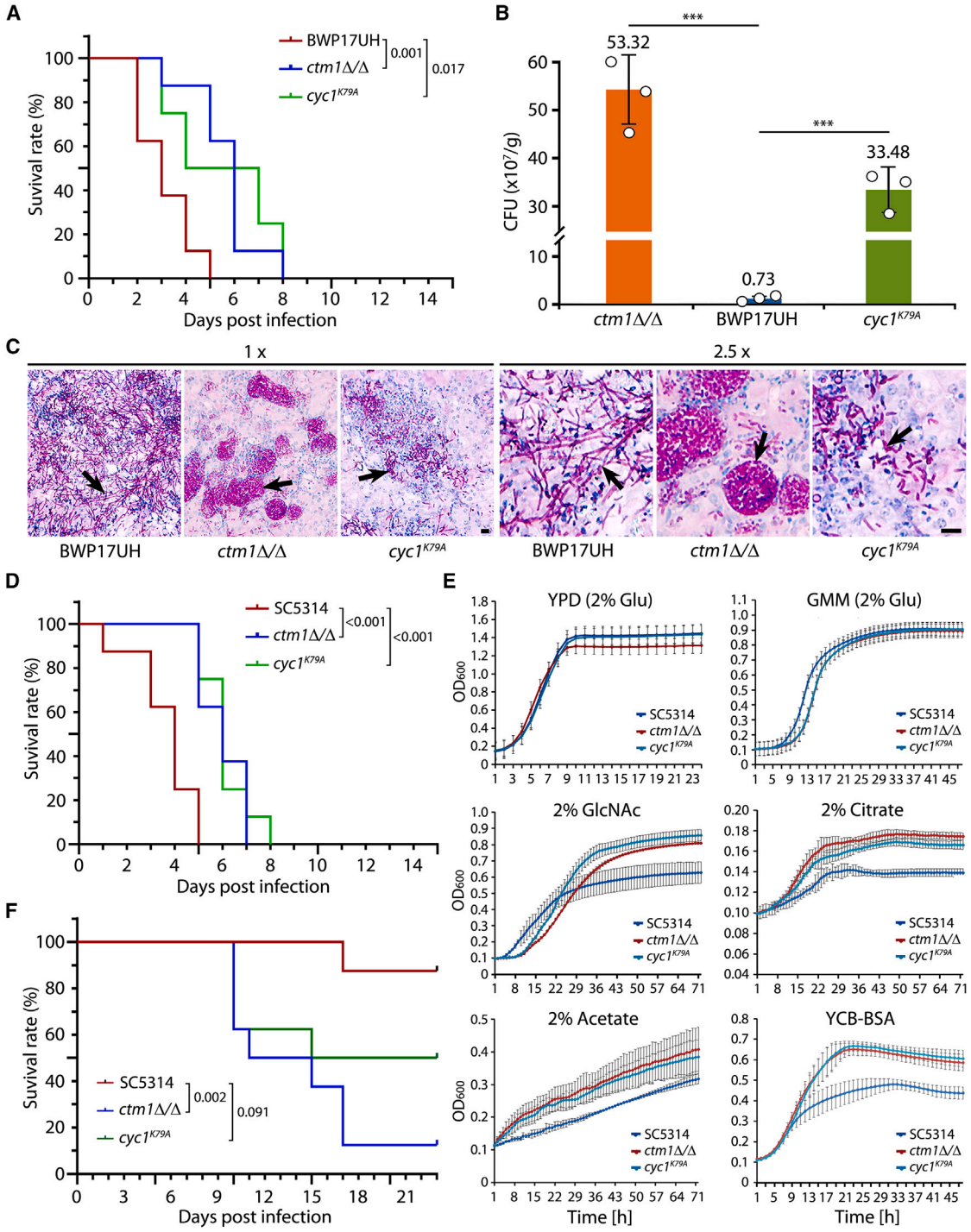


**Figure 6. *ctm1*Δ/Δ and *cyc1*$^{K79A}$ mutants exhibit full virulence and accelerated proliferation**

(A) Virulence of BWP17UH, *ctm1*Δ/Δ (GZY1275), and *cyc1*$^{K79A}$ (GZY1314) in the mouse model of systemic infection.

(B) Fungal burden in the kidneys of mice infected with BWP17UH, *ctm1*Δ/Δ, and *cyc1*$^{K79A}$. Kidneys were harvested at 48 h post infection, weighed, and homogenized for enumeration of CFUs. The two-tailed student's t test was used to check statistical significances, and p values are indicated by asterisks (***p ≤ 0.001).

(C) Histopathologic examination of kidneys from mice infected with BWP17UH, *ctm1*Δ/Δ, and *cyc1*$^{K79A}$. Kidneys were harvested at 48 h post infection and sectioned for staining with periodic acid-Schiff (PAS) reagent using standard procedures. Arrows indicate *C. albicans* cells. Bars, 20 μm.

(D) Virulence of SC5314, *ctm1*Δ/Δ (GZY1423), and *cyc1*$^{K79A}$ (GZY1454) in the mouse model of systemic infection.

*(legend continued on next page)*

Considering that the use of the *URA3* marker for gene disruption may affect the accuracy of virulence assays,[53,54] we further generated new *ctm1*Δ/Δ and *cyc1*$^{K79A}$ mutants using the *SAT1* flipper system in the clinical isolate SC5314. Using these strains produced similar results in the repeated virulence assays (Figure 6D).

A recent study demonstrated that the filament-deficient *eed1*Δ/Δ mutant remained fully virulent during systemic infection of mice due to rapid proliferation resulting from better metabolic adaptation.[18] To investigate whether the same mechanism underlies the virulence of *ctm1*Δ/Δ and *cyc1*$^{K79A}$, we measured their growth curves in comparison with WT (SC5314) in different media. *ctm1*Δ/Δ and *cyc1*$^{K79A}$ exhibited similar growth curves to WT in YPD and Glucose Minimum Media (GMM) containing 2% glucose (Figure 6E). However, both mutants showed faster growth than WT in media containing physiologically relevant carbon sources such as acetate, citrate, and GlcNAc, and in the YCB-BSA medium (Figure 6E). The faster-than-WT growth of the mutants in media mimicking physiologically relevant nutrient supply reflects the mutants' better metabolic adaptation.

The *eed1*Δ/Δ mutant exhibited higher virulence than WT when low infectious doses were used.[18] Similarly, both *ctm1*Δ/Δ and *cyc1*$^{K79A}$ were more virulent than WT when the infection dose was reduced to 2 × $10^4$ cells per mouse. On days 11 and 15 after inoculation, 50% of mice infected with *ctm1*Δ/Δ or *cyc1*$^{K79A}$ had died, respectively. In contrast, all mice infected with WT remained alive until day 17. By the end of observation (day 23), the survival rates were 20%, 50%, and 80% for mice infected with *ctm1*Δ/Δ, *cyc1*$^{K79A}$, and WT, respectively (Figure 6F).

Taken together, these data suggest that blocking Cyc1 methylation results in better metabolic adaptation and faster proliferation of *C. albicans* during systemic infection, which compensates for the loss of pathogenic traits associated with hyphal growth to maintain virulence.

## DISCUSSION

This study reports that inactivating *CTM1* prevents hyphal development in *C. albicans*. Ctm1 trimethylates Cyc1 at K79, and deletion of *CTM1* produces unmethylated Cyc1. Cyc1$^{UnM}$ associates with PKA's catalytic subunits and inhibits their kinase activity, thus blocking cAMP-PKA signaling and hyphal morphogenesis. Strikingly, the hypha-deficient *ctm1*Δ/Δ and *cyc1*$^{K79A}$ mutants exhibit high virulence during systemic infection of mice. They grew markedly faster than WT in the infected mice and in media containing physiologically relevant nutrients, indicating robust metabolic adaptation. Together, our findings have revealed a crucial role for Cyt-C in regulating virulence-related traits in *C. albicans*. This study also demonstrates a cellular function for Cyt-C methylation, which is evolutionarily conserved in fungi and plants.

The recent isolation of haploid *C. albicans* strains has empowered researchers with powerful genetic tools for conducting genome-scale genetic studies of this pathogen.[37,55–58] As a result, many genes involved in azole resistance,[37] biofilm formation,[59] amphotericin B resistance,[60] white-opaque switch,[61] mechanism of action of antifungal agents,[62] and antifungal susceptibility[63] have been discovered. In this study, we utilized haploid *C. albicans* to conduct genetic screens and identified genes and mechanisms governing the yeast-hyphal transition. These exciting results should encourage scientists to incorporate haploid *C. albicans* into future research.

The trimethylation of a lysine residue equivalent to K79 on Cyt-C of *C. albicans* is evolutionarily conserved in plants and fungi, seemingly involving a dedicated methyltransferase.[32–35] From an evolutionary standpoint, this specific modification is expected to play an important role in plants and fungi. However, to date, studies in *S. cerevisiae* have not definitively revealed any function of Cyt-C's methylation.[36] While our results exclude a role for Cyc1 methylation in electron transport in *C. albicans*, they unveil the evolution of a specific role for Cyto-C methylation in the regulation of hyphal growth in *C. albicans*. This conclusion is supported by the following observations. First, deletion of *CTM1* blocks both Cyc1 methylation and hyphal growth. Second, cells expressing Cyc1$^{K79A}$ fail to grow hyphae. Third, *ctm1*Δ/Δ and *cyc1*$^{K79A}$ produce lower levels of HSGs and higher levels of *NRG1*. Last, Cyc1$^{UnM}$ binds to the catalytic subunits of PKA, inhibiting their kinase activity. Collectively, our discoveries demonstrate a role for Cyc1$^{UnM}$ in inhibiting *C. albicans* hyphal growth, revealing a biological function of Cyt-C methylation.

We propose that the primary function of Ctm1 trimethylation on Cyc1 is to regulate the yeast-to-hypha transition in hyphal growth. We found that the methylation level of Cyc1 is dynamic and can be affected by growth conditions, correlating with the extent of filamentation. However, what determines the methylation level of Cyc1 remains unclear. A cell may achieve this by regulating the cellular level of Ctm1 or its methylase activity. Another possibility is the involvement of lysine demethylases. In many organisms, a family of lysine demethylases regulates lysine methylation levels on histones.[64] Cyc1 may also be subject to a similar mechanism. However, specific demethylases for Cyto-C have not yet been identified in *C. albicans*.

Yeast Cyto-C is synthesized in cytoplasm as the apo-form and sequentially modified by lysine methylation and heme attachment during transportation into the mitochondrial intermembrane space to become the mature holoprotein.[65] As Cyc1$^{UnM}$ is fully functional in electron transport, the deletion of *CTM1* seems not to affect the formation of holo-Cyc1. However, it is possible that *ctm1*Δ/Δ may slow down the maturation progress, leading to an increase in the cytoplasmic accumulation of apo-Cyc1 and a reduction of the level of holo-Cyc1 in the

(E) Growth measurement of SC5314, *ctm1*Δ/Δ, and *cyc1*$^{K79A}$. Cells were cultured in each medium as indicated at 30°C overnight. The cultures were diluted to $OD_{600}$ = 0.1 and aliquoted to a 96-well microplate. The plate was incubated at 37°C and cell growth was recorded by measuring $OD_{600}$ with a microplate reader at 1-h intervals for up to 72 h. Graphs show the mean ± SD of three independent biological replicates.
(F) Virulence of SC5314, *ctm1*Δ/Δ, and *cyc1*$^{K79A}$ in the mouse model of systemic infection at low infectious dose. For virulence analysis, each of the 8- to 10-week-old BALB/c mice (n = 8 per group) was injected via the tail vein with 8 × $10^5$ (A and D) or 2 × $10^4$ (F) cells of a strain. Survival was monitored over a course of 15 (A and D) or 23 (F) days and is shown as Kaplan-Meyer curves. Survival curves were compared using the two-sided log rank (Mantel-Cox) test and p valves are shown in the graphs.

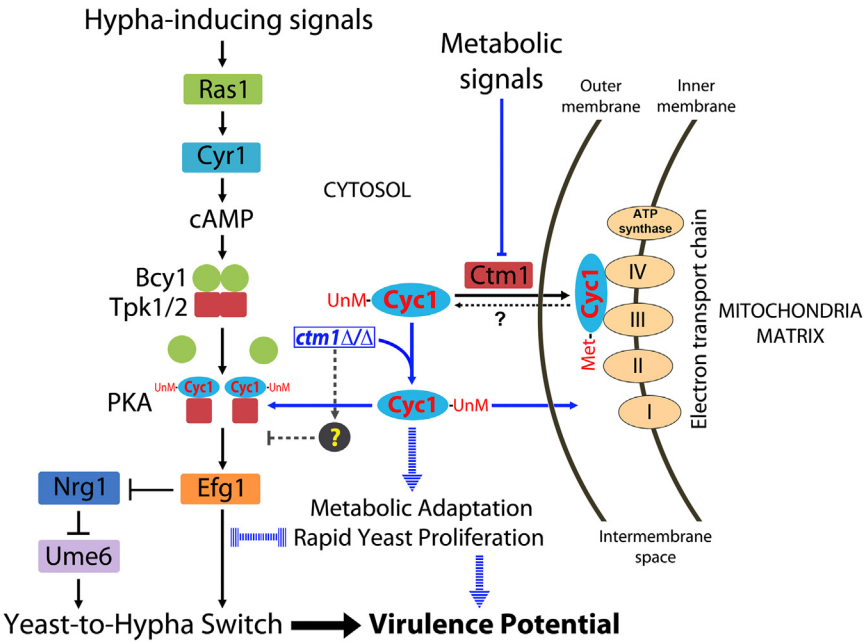


**Figure 7. A model depicting how Ctm1 and Cyc1 regulate the hyphal morphogenesis of *C. albicans***

The cAMP-PKA signaling pathways that control *NRG1* and HSG expression are shown on the left and the complexes of ETC located on the mitochondrial inner membrane are shown on the right. Ctm1 trimethylates Cyc1 on K79. While both methylated and unmethylated Cyc1 can enter mitochondria to take part in electron transport, unmethylated Cyc1 also binds to PKA and inhibits the kinase activity, leading to the suppression of hyphal morphogenesis. Environmental conditions can influence the methylation level of Cyc1, probably via modulating the amount and/or enzyme activity of Ctm1 or other mechanisms such as demethylation by unidentified demethylase(s). However, what controls Ctm1 activity and Cyc1 demethylation remains unknown. Under certain circumstances, such as in the host kidney, unmethylated Cyc1 also triggers metabolic reprogramming for adaptation to nutrient availability to accelerate the proliferation of *C. albicans* in the yeast form to maintain virulence. In addition to Cyc1, one or more Ctm1 downstream targets may function in parallel to suppress hyphal growth in *ctm1*Δ/Δ cells.

mitochondria. Although we could detect Cyc1 in both the cytoplasm and mitochondria in *C. albicans* by microscopic and biochemical methods, we were unable to compare their ratio changes due to the lack of proper internal controls.

The observation of Cyc1 cytoplasmic localization suggests that Cyt-C has evolved specific functions in the cytosol in fungi. Indeed, we detected specific interaction between Cyc1$^{UnM}$ and PKA, which inhibits PKA's kinase activity and blocks cAMP-PKA signaling. Additionally, these findings identify a cellular function for the methylation and demethylation of Cyt-C in a fungal species, which takes place in the cytosol rather than in the mitochondria. This knowledge could be very important because cAMP-PKA signaling determines the virulence of many pathogenic fungi.[66–69] It would be interesting to determine whether the regulation of PKA by unmethylated Cyt-C is conserved in other fungi.

Mitochondrial activity and metabolic state influence the hyphal growth of *C. albicans*.[23,24,26,70] Recently, the mitochondrion has been proposed to function as a metabolic checkpoint for hyphal growth.[26] Could Cyc1 be a key component of this checkpoint? Our studies do not provide direct evidence that changes in any mitochondrial activity affect hyphal growth. However, they reveal a correlation between nutrient sources, Cyc1 methylation levels, and hyphal growth. We hypothesize that some specific metabolic or stress signals in the mitochondria may trigger Ctm1 methylation or demethylation mechanisms to determine the ratio between Cyc1$^{UnM}$ and Cyc1$^{Met}$ (methylated Cyc1). This, in turn, governs the dynamic shifting between yeast growth and hyphal growth in *C. albicans*. This regulation is achieved, at least partly, through Cyc1$^{UnM}$'s inhibitory association with PKA to block cAMP/PKA signaling. During the immunopurification of Cyc1 and Tpk1/2 for *in vitro* kinase assays, we observed that Cyc1 is much more abundant than Tpk1/2. Therefore, a small increase in the cellular level of unmethylated Cyc1 could be sufficient to cause a substantial inhibition of PKA activity, making this reversible regulation sensitive and dynamic.

During the systemic infection of mice, *ctm1*Δ/Δ and *cyc1*$^{K79A}$ remain virulent, causing even faster mortality than WT at low infectious doses. Several organs of mice infected with *ctm1*Δ/Δ and *cyc1*$^{K79A}$ exhibited a fungal burden many times higher than those infected with the WT strain, indicating an enhanced ability of *ctm1*Δ/Δ and *cyc1*$^{K79A}$ to colonize and proliferate in the host. However, this may not necessarily arise from the inhibition of PKA by Cyc1$^{UnM}$, as some hyphae-defective mutants, such as the cyr1 mutant, with downregulated PKA signaling exhibited reduced virulence,[46] which is an important issue requiring further investigation. To our knowledge, the only reported hyphae-defective mutant exhibiting a similar phenotype to *ctm1*Δ/Δ and *cyc1*$^{K79A}$ is *eed1*Δ/Δ.[18] All three mutants grew faster than WT in media containing physiologically relevant nutrients, indicating their ability to adapt metabolically to improve fitness during systemic host infection, compensating for the loss of invasive hyphal growth to maintain virulence. We propose that robust hyphal growth and accelerated yeast proliferation are two complementary strategies *C. albicans* has evolved to maintain full virulence. The dynamic shift between the two strategies allows *C. albicans* to navigate diverse host niches with varying nutrient supplies without compromising infection capabilities.

By interfering with cAMP-PKA signaling, Cyc1$^{UnM}$ plays a key role in inhibiting the hyphal morphogenesis and possibly increasing yeast proliferation (Figure 7). Interestingly, we found that the absence of Cyc1$^{UnM}$ failed to suppress the hyphal deficiency of *ctm1*Δ/Δ, as most *ctm1*Δ/Δ *cyc1*Δ/Δ cells grew as yeast during hyphal induction (Figure S5A), suggesting the existence of other Ctm1 downstream target(s) that functions in parallel with Cyc1$^{UnM}$ to suppress hyphal growth in

*ctm1*Δ/Δ (Figure 7). We hypothesize that, in *ctm1*Δ/Δ cells, either of two parallel pathways can suppress hyphal growth: one through $Cyc1^{UnM}$ and another as-yet unidentified mechanism. In the absence of Ctm1, both pathways are activated, while, in *ctm1*Δ/Δ *cyc1*Δ/Δ cells, $Cyc1^{UnM}$ is missing, thereby compromising the suppressing activity. Supporting this hypothesis, we found that *ctm1*Δ/Δ *cyc1*Δ/Δ cells tended to produce many more elongated buds and hyphae than *ctm1*Δ/Δ under enhanced hyphal-inducing conditions (Figure S5B). Moreover, we have observed the more pronounced downregulation of HSGs and upregulation of *NRG1* in *ctm1*Δ/Δ than in $Cyc1^{UnM}$, as well as the higher fungal burdens of *ctm1*Δ/Δ than $Cyc1^{UnM}$ in infected mice. Currently, the identity of other putative Ctm1 target(s) remains unknown. Nevertheless, this study has elucidated one pathway for suppressing hyphal growth downstream of *CTM1*.

Our findings open opportunities for future research to map out the molecular details about how *C. albicans* uses Cyc1 to orchestrate growth mode selection, cell proliferation, and metabolism, ensuring proliferation and pathogenicity within the host. It would also be interesting to investigate whether other fungal pathogens employ similar strategies to regulate virulence. This knowledge will offer valuable insights for developing effective antifungal therapeutics against invasive fungal diseases. Additionally, since mitochondria are central to metabolism and are associated with metabolic disorders[71,72] and cancer,[71,73] our discovery of Cyto-C balancing metabolism and cell proliferation may have broader implications for human metabolic diseases.

### Limitations of the study

This study has a couple of limitations. First, while we have detected dynamic changes in the cellular level of methylated Cyc1 under different growth conditions by WB using an antibody that specifically recognizes trimethylated lysine, accurately determining the ratio between $Cyc1^{Met}$ and $Cyc1^{UnM}$ remains challenging due to the lack of appropriate methods. MS is one possible means that could potentially address this issue. Second, our data suggest the existence of more than one target or pathway downstream of Ctm1 that functions in parallel to suppress hyphal growth in *ctm1*Δ/Δ mutants. However, we have only identified Cyc1 as a direct substrate of Ctm1 and established the essentiality of Ctm1 methylation of Cyc1 at K79 for hyphal growth. A global proteomic comparison using MS to analyze trimethylated proteins in WT and *ctm1*Δ/Δ cells may help identify additional Ctm1 targets. Further studies of these proteins will lead to a more comprehensive understanding of hyphal regulation by Ctm1.

## STAR★METHODS

Detailed methods are provided in the online version of this paper and include the following:

- KEY RESOURCES TABLE
- RESOURCE AVAILABILITY
  - Lead contact
  - Materials availability
  - Data and code availability
- EXPERIMENTAL MODEL AND STUDY PARTICIPANT DETAILS
  - Bacteria strains
  - *C. albicans* strains
  - Mouse lines
- METHOD DETAILS
  - DNA manipulation and transformation
  - Transposon-mediated insertional haploid mutant library
  - RNA extraction, cDNA preparation, and qRT-PCR
  - RNA-seq and data analysis
  - Protein extraction, IP, and WB
  - Differential fractionation of yeast mitochondria and cytosol
  - Immunopurification and *in vitro* PKA kinase assay
  - Mass spectrometry (MS) analysis
  - Optical and fluorescent microscopy
  - Growth curve measurement
  - Virulence analysis
  - Histopathology and CFU counting
  - Fungal burden measurement by qPCR
- QUANTIFICATION AND STATISTICAL ANALYSIS

### SUPPLEMENTAL INFORMATION

Supplemental information can be found online at https://doi.org/10.1016/j.celrep.2023.113473.

### ACKNOWLEDGMENTS

This work was supported by grants from National Medical Research Council of Singapore (NMRC), National Research Foundation of Singapore (NRF), A*STAR Biomedical Research Council (BMRC), and A*STAR Horizontal Technology Programme Offices (HTPO) (NMRC/OFIRG/0055/2019, HTPO SEED_ID_IMCB_C211418006, NRF-ISF003-3039, and NMRC/OFIRG21jun-0058 to Y.W. and BMRC042 to G.Z.). Graphical abstract was created with BioRender.

### AUTHOR CONTRIBUTIONS

G.Z., experimental design, conducting experiments, data analysis, and preparation of the manuscript; X.Z.B. and Y.J.K., MS experiments and data analysis; X.X., animal experiments; F.S.D., qRT-PCR and data analysis; E.W.L.C., genetic screen for hyphae-defective mutants; J.G., construction of the host haploid strain for the transposon-insertion mutant library; and Y.W., experimental design, supervision of the project, funding acquisition, and writing the manuscript.

### DECLARATION OF INTERESTS

The authors declare no competing interests.

Received: June 19, 2023
Revised: October 17, 2023
Accepted: November 6, 2023
Published: November 18, 2023

### REFERENCES

1. Hallen-Adams, H.E., and Suhr, M.J. (2017). Fungi in the healthy human gastrointestinal tract. Virulence *8*, 352–358.
2. Cleveland, A.A., Farley, M.M., Harrison, L.H., Stein, B., Hollick, R., Lockhart, S.R., Magill, S.S., Derado, G., Park, B.J., and Chiller, T.M. (2012). Changes in incidence and antifungal drug resistance in

candidemia: results from population-based laboratory surveillance in Atlanta and Baltimore, 2008-2011. Clin. Infect. Dis. *55*, 1352–1361.

3. Brown, G.D., Denning, D.W., Gow, N.A.R., Levitz, S.M., Netea, M.G., and White, T.C. (2012). Hidden killers: human fungal infections. Sci. Transl. Med. *4*, 165rv13.
4. Aslam, B., Wang, W., Arshad, M.I., Khurshid, M., Muzammil, S., Rasool, M.H., Nisar, M.A., Alvi, R.F., Aslam, M.A., Qamar, M.U., et al. (2018). Antibiotic resistance: a rundown of a global crisis. Infect. Drug Resist. *11*, 1645–1658.
5. Sudbery, P., Gow, N., and Berman, J. (2004). The distinct morphogenic states of Candida albicans. Trends Microbiol. *12*, 317–324.
6. Sudbery, P.E. (2011). Growth of Candida albicans hyphae. Nat. Rev. Microbiol. *9*, 737–748.
7. de Groot, P.W.J., Bader, O., de Boer, A.D., Weig, M., and Chauhan, N. (2013). Adhesins in human fungal pathogens: glue with plenty of stick. Eukaryot. Cell *12*, 470–481.
8. Ramos, L.S., Branquinha, M.H., and Santos, A.L.S. (2017). Different classes of hydrolytic enzymes produced by multidrug-resistant yeasts comprising the Candida haemulonii complex. Med. Mycol. *55*, 228–232.
9. Moyes, D.L., Wilson, D., Richardson, J.P., Mogavero, S., Tang, S.X., Wernecke, J., Höfs, S., Gratacap, R.L., Robbins, J., Runglall, M., et al. (2016). Candidalysin is a fungal peptide toxin critical for mucosal infection. Nature *532*, 64–68.
10. Westman, J., Hube, B., and Fairn, G.D. (2019). Integrity under stress: Host membrane remodelling and damage by fungal pathogens. Cell Microbiol. *21*, e13016.
11. Bar-Yosef, H., Vivanco Gonzalez, N., Ben-Aroya, S., Kron, S.J., and Kornitzer, D. (2017). Chemical inhibitors of Candida albicans hyphal morphogenesis target endocytosis. Sci. Rep. *7*, 5692.
12. Romo, J.A., Pierce, C.G., Chaturvedi, A.K., Lazzell, A.L., McHardy, S.F., Saville, S.P., and Lopez-Ribot, J.L. (2017). Development of Anti-Virulence Approaches for Candidiasis via a Novel Series of Small-Molecule Inhibitors of Candida albicans Filamentation. mBio *8*, e01991-17.
13. Biswas, S., Van Dijck, P., and Datta, A. (2007). Environmental sensing and signal transduction pathways regulating morphopathogenic determinants of Candida albicans. Microbiol. Mol. Biol. Rev. *71*, 348–376.
14. Carlisle, P.L., and Kadosh, D. (2013). A genome-wide transcriptional analysis of morphology determination in Candida albicans. Mol. Biol. Cell *24*, 246–260.
15. Wang, Y. (2013). Fungal adenylyl cyclase acts as a signal sensor and integrator and plays a central role in interaction with bacteria. PLoS Pathog. *9*, e1003612.
16. Pellon, A., Begum, N., Sadeghi Nasab, S.D., Harzandi, A., Shoaie, S., and Moyes, D.L. (2022). Role of Cellular Metabolism during Candida-Host Interactions. Pathogens *11*, 184.
17. Burgain, A., Tebbji, F., Khemiri, I., and Sellam, A. (2020). Metabolic Reprogramming in the Opportunistic Yeast Candida albicans in Response to Hypoxia. mSphere *5*, e00913-19.
18. Dunker, C., Polke, M., Schulze-Richter, B., Schubert, K., Rudolphi, S., Gressler, A.E., Pawlik, T., Prada Salcedo, J.P., Niemiec, M.J., Slesiona-Künzel, S., et al. (2021). Rapid proliferation due to better metabolic adaptation results in full virulence of a filament-deficient Candida albicans strain. Nat. Commun. *12*, 3899.
19. Mamouei, Z., Zeng, G., Wang, Y.M., and Wang, Y. (2017). Candida albicans possess a highly versatile and dynamic high-affinity iron transport system important for its commensal-pathogenic lifestyle. Mol. Microbiol. *106*, 986–998.
20. Nemoto, S., Takeda, K., Yu, Z.X., Ferrans, V.J., and Finkel, T. (2000). Role for mitochondrial oxidants as regulators of cellular metabolism. Mol. Cell Biol. *20*, 7311–7318.
21. Chandel, N.S. (2014). Mitochondria as signaling organelles. BMC Biol. *12*, 34.
22. Calderone, R., Li, D., and Traven, A. (2015). System-level impact of mitochondria on fungal virulence: to metabolism and beyond. FEMS Yeast Res. *15*, fov027.
23. Grahl, N., Demers, E.G., Lindsay, A.K., Harty, C.E., Willger, S.D., Piispanen, A.E., and Hogan, D.A. (2015). Mitochondrial Activity and Cyr1 Are Key Regulators of Ras1 Activation of C. albicans Virulence Pathways. PLoS Pathog. *11*, e1005133.
24. Huang, X., Chen, X., He, Y., Yu, X., Li, S., Gao, N., Niu, L., Mao, Y., Wang, Y., Wu, X., et al. (2017). Mitochondrial complex I bridges a connection between regulation of carbon flexibility and gastrointestinal commensalism in the human fungal pathogen Candida albicans. PLoS Pathog. *13*, e1006414.
25. Watanabe, T., Ogasawara, A., Mikami, T., and Matsumoto, T. (2006). Hyphal formation of Candida albicans is controlled by electron transfer system. Biochem. Biophys. Res. Commun. *348*, 206–211.
26. Koch, B., Barugahare, A.A., Lo, T.L., Huang, C., Schittenhelm, R.B., Powell, D.R., Beilharz, T.H., and Traven, A. (2018). A Metabolic Checkpoint for the Yeast-to-Hyphae Developmental Switch Regulated by Endogenous Nitric Oxide Signaling. Cell Rep. *25*, 2244–2258.e7.
27. Hoogenraad, N.J., Ward, L.A., and Ryan, M.T. (2002). Import and assembly of proteins into mitochondria of mammalian cells. Biochim. Biophys. Acta *1592*, 97–105.
28. Salemme, F.R. (1977). Structure and function of cytochromes c. Annu. Rev. Biochem. *46*, 299–329.
29. Kluck, R.M., Bossy-Wetzel, E., Green, D.R., and Newmeyer, D.D. (1997). The release of cytochrome c from mitochondria: a primary site for Bcl-2 regulation of apoptosis. Science *275*, 1132–1136.
30. Alvarez-Paggi, D., Hannibal, L., Castro, M.A., Oviedo-Rouco, S., Demicheli, V., Tórtora, V., Tomasina, F., Radi, R., and Murgida, D.H. (2017). Multifunctional Cytochrome c: Learning New Tricks from an Old Dog. Chem. Rev. *117*, 13382–13460.
31. Polevoda, B., Martzen, M.R., Das, B., Phizicky, E.M., and Sherman, F. (2000). Cytochrome c methyltransferase, Ctm1p, of yeast. J. Biol. Chem. *275*, 20508–20513.
32. DeLange, R.J., Glazer, A.N., and Smith, E.L. (1969). Presence and location of an unusual amino acid, epsilon-N-trimethyllysine, in cytochrome c of wheat germ and Neurospora. J. Biol. Chem. *244*, 1385–1388.
33. Brown, R.H., and Boulter, D. (1973). The amino acid sequence of cytochrome c from Nigella damascena L. (love-in-a-mist). Biochem. J. *133*, 251–254.
34. DeLange, R.J., Glazer, A.N., and Smith, E.L. (1970). Identification and location of episilon-N-trimethyllysine in yeast cytochromes c. J. Biol. Chem. *245*, 3325–3327.
35. Sugeno, K., Narita, K., and Titani, K. (1971). The amino acid sequence of cytochrome c from Debaryomyces kloeckeri. J. Biochem. *70*, 659–682.
36. Cessay, K.J., Bergman, L.W., and Tuck, M.T. (1991). Further investigations regarding the role of trimethyllysine for cytochrome c uptake into mitochondria. Int. J. Biochem. *23*, 761–768.
37. Gao, J., Wang, H., Li, Z., Wong, A.H.H., Wang, Y.Z., Guo, Y., Lin, X., Zeng, G., Liu, H., Wang, Y., and Wang, J. (2018). Candida albicans gains azole resistance by altering sphingolipid composition. Nat. Commun. *9*, 4495.
38. Hatefi, Y. (1985). The mitochondrial electron transport and oxidative phosphorylation system. Annu. Rev. Biochem. *54*, 1015–1069.
39. Turcotte, B., Liang, X.B., Robert, F., and Soontorngun, N. (2010). Transcriptional regulation of nonfermentable carbon utilization in budding yeast. FEMS Yeast Res. *10*, 2–13.
40. Murad, A.M., Leng, P., Straffon, M., Wishart, J., Macaskill, S., MacCallum, D., Schnell, N., Talibi, D., Marechal, D., Tekaia, F., et al. (2001). NRG1 represses yeast-hypha morphogenesis and hypha-specific gene expression in Candida albicans. EMBO J. *20*, 4742–4752.
41. Braun, B.R., Kadosh, D., and Johnson, A.D. (2001). NRG1, a repressor of filamentous growth in C.albicans, is down-regulated during filament induction. EMBO J. *20*, 4753–4761.

42. Lu, Y., Su, C., Unoje, O., and Liu, H. (2014). Quorum sensing controls hyphal initiation in Candida albicans through Ubr1-mediated protein degradation. Proc. Natl. Acad. Sci. USA *111*, 1975–1980.

43. Bockmühl, D.P., and Ernst, J.F. (2001). A potential phosphorylation site for an A-type kinase in the Efg1 regulator protein contributes to hyphal morphogenesis of Candida albicans. Genetics *157*, 1523–1530.

44. Lu, Y., Su, C., Wang, A., and Liu, H. (2011). Hyphal development in Candida albicans requires two temporally linked changes in promoter chromatin for initiation and maintenance. PLoS Biol. *9*, e1001105.

45. Scott, J.D. (1991). Cyclic nucleotide-dependent protein kinases. Pharmacol. Ther. *50*, 123–145.

46. Rocha, C.R., Schröppel, K., Harcus, D., Marcil, A., Dignard, D., Taylor, B.N., Thomas, D.Y., Whiteway, M., and Leberer, E. (2001). Signaling through adenylyl cyclase is essential for hyphal growth and virulence in the pathogenic fungus Candida albicans. Mol. Biol. Cell *12*, 3631–3643.

47. Griffioen, G., Anghileri, P., Imre, E., Baroni, M.D., and Ruis, H. (2000). Nutritional control of nucleocytoplasmic localization of cAMP-dependent protein kinase catalytic and regulatory subunits in Saccharomyces cerevisiae. J. Biol. Chem. *275*, 1449–1456.

48. Cassola, A., Parrot, M., Silberstein, S., Magee, B.B., Passeron, S., Giasson, L., and Cantore, M.L. (2004). Candida albicans lacking the gene encoding the regulatory subunit of protein kinase A displays a defect in hyphal formation and an altered localization of the catalytic subunit. Eukaryot. Cell *3*, 190–199.

49. Ghaemmaghami, S., Huh, W.K., Bower, K., Howson, R.W., Belle, A., Dephoure, N., O'Shea, E.K., and Weissman, J.S. (2003). Global analysis of protein expression in yeast. Nature *425*, 737–741.

50. Huh, W.K., Falvo, J.V., Gerke, L.C., Carroll, A.S., Howson, R.W., Weissman, J.S., and O'Shea, E.K. (2003). Global analysis of protein localization in budding yeast. Nature *425*, 686–691.

51. Boldogh, I.R., and Pon, L.A. (2007). Purification and subfractionation of mitochondria from the yeast Saccharomyces cerevisiae. Methods Cell Biol. *80*, 45–64.

52. Bowman, J.C., Abruzzo, G.K., Anderson, J.W., Flattery, A.M., Gill, C.J., Pikounis, V.B., Schmatz, D.M., Liberator, P.A., and Douglas, C.M. (2001). Quantitative PCR assay to measure Aspergillus fumigatus burden in a murine model of disseminated aspergillosis: demonstration of efficacy of caspofungin acetate. Antimicrob. Agents Chemother. *45*, 3474–3481.

53. Lay, J., Henry, L.K., Clifford, J., Koltin, Y., Bulawa, C.E., and Becker, J.M. (1998). Altered expression of selectable marker URA3 in gene-disrupted Candida albicans strains complicates interpretation of virulence studies. Infect. Immun. *66*, 5301–5306.

54. Brand, A., MacCallum, D.M., Brown, A.J.P., Gow, N.A.R., and Odds, F.C. (2004). Ectopic expression of URA3 can influence the virulence phenotypes and proteome of Candida albicans but can be overcome by targeted reintegration of URA3 at the RPS10 locus. Eukaryot. Cell *3*, 900–909.

55. Hickman, M.A., Zeng, G., Forche, A., Hirakawa, M.P., Abbey, D., Harrison, B.D., Wang, Y.M., Su, C.H., Bennett, R.J., Wang, Y., and Berman, J. (2013). The 'obligate diploid' Candida albicans forms mating-competent haploids. Nature *494*, 55–59.

56. Zeng, G., Wang, Y.M., Chan, F.Y., and Wang, Y. (2014). One-step targeted gene deletion in Candida albicans haploids. Nat. Protoc. *9*, 464–473.

57. Shapiro, R.S., Chavez, A., Porter, C.B.M., Hamblin, M., Kaas, C.S., DiCarlo, J.E., Zeng, G., Xu, X., Revtovich, A.V., Kirienko, N.V., et al. (2018). A CRISPR-Cas9-based gene drive platform for genetic interaction analysis in Candida albicans. Nat. Microbiol. *3*, 73–82.

58. Mielich, K., Shtifman-Segal, E., Golz, J.C., Zeng, G., Wang, Y., Berman, J., and Kunze, R. (2018). Maize Transposable Elements Ac/Ds as Insertion Mutagenesis Tools in Candida albicans. G3 (Bethesda) *8*, 1139–1145.

59. Seneviratne, C.J., Zeng, G., Truong, T., Sze, S., Wong, W., Samaranayake, L., Chan, F.Y., Wang, Y.M., Wang, H., Gao, J., and Wang, Y. (2015). New "haploid biofilm model" unravels IRA2 as a novel regulator of Candida albicans biofilm formation. Sci. Rep. *5*, 12433.

60. Truong, T., Zeng, G., Qingsong, L., Kwang, L.T., Tong, C., Chan, F.Y., Wang, Y., and Seneviratne, C.J. (2016). Comparative Ploidy Proteomics of Candida albicans Biofilms Unraveled the Role of the AHP1 Gene in the Biofilm Persistence Against Amphotericin B. Mol. Cell. Proteomics *15*, 3488–3500.

61. Yang, S.L., Zeng, G., Chan, F.Y., Wang, Y.M., Yang, D., and Wang, Y. (2018). Sac7 and Rho1 regulate the white-to-opaque switching in Candida albicans. Sci. Rep. *8*, 875.

62. Truong, T., Suriyanarayanan, T., Zeng, G., Le, T.D., Liu, L., Li, J., Tong, C., Wang, Y., and Seneviratne, C.J. (2018). Use of Haploid Model of Candida albicans to Uncover Mechanism of Action of a Novel Antifungal Agent. Front. Cell. Infect. Microbiol. *8*, 164.

63. Truong, T., Zeng, G., Lim, T.K., Cao, T., Pang, L.M., Lee, Y.M., Lin, Q., Wang, Y., and Seneviratne, C.J. (2020). Proteomics Analysis of Candida albicans dnm1 Haploid Mutant Unraveled the Association between Mitochondrial Fission and Antifungal Susceptibility. Proteomics *20*, e1900240.

64. Tsukada, Y.i., Fang, J., Erdjument-Bromage, H., Warren, M.E., Borchers, C.H., Tempst, P., and Zhang, Y. (2006). Histone demethylation by a family of JmjC domain-containing proteins. Nature *439*, 811–816.

65. Sherman, F. (1990). Studies of yeast cytochrome c: how and why they started and why they continued. Genetics *125*, 9–12.

66. Choi, J., Jung, W.H., and Kronstad, J.W. (2015). The cAMP/protein kinase A signaling pathway in pathogenic basidiomycete fungi: Connections with iron homeostasis. J. Microbiol. *53*, 579–587.

67. Lin, C.J., and Chen, Y.L. (2018). Conserved and Divergent Functions of the cAMP/PKA Signaling Pathway in Candida albicans and Candida tropicalis. J. Fungi *4*, 68.

68. Caza, M., and Kronstad, J.W. (2019). The cAMP/Protein Kinase a Pathway Regulates Virulence and Adaptation to Host Conditions in Cryptococcus neoformans. Front. Cell. Infect. Microbiol. *9*, 212.

69. Huang, G., Huang, Q., Wei, Y., Wang, Y., and Du, H. (2019). Multiple roles and diverse regulation of the Ras/cAMP/protein kinase A pathway in Candida albicans. Mol. Microbiol. *111*, 6–16.

70. Silao, F.G.S., Ward, M., Ryman, K., Wallström, A., Brindefalk, B., Udekwu, K., and Ljungdahl, P.O. (2019). Mitochondrial proline catabolism activates Ras1/cAMP/PKA-induced filamentation in Candida albicans. PLoS Genet. *15*, e1007976.

71. McInnes, J. (2013). Mitochondrial-associated metabolic disorders: foundations, pathologies and recent progress. Nutr. Metab. *10*, 63.

72. Prasun, P. (2020). Mitochondrial dysfunction in metabolic syndrome. Biochim. Biophys. Acta, Mol. Basis Dis. *1866*, 165838.

73. Porporato, P.E., Filigheddu, N., Pedro, J.M.B.S., Kroemer, G., and Galluzzi, L. (2018). Mitochondrial metabolism and cancer. Cell Res. *28*, 265–280.

74. Morschhäuser, J., Michel, S., and Staib, P. (1999). Sequential gene disruption in Candida albicans by FLP-mediated site-specific recombination. Mol. Microbiol. *32*, 547–556.

75. Wiśniewski, J.R., Zougman, A., Nagaraj, N., and Mann, M. (2009). Universal sample preparation method for proteome analysis. Nat. Methods *6*, 359–362.

## STAR★METHODS

### KEY RESOURCES TABLE

| REAGENT or RESOURCE | SOURCE | IDENTIFIER |
|---|---|---|
| Antibodies | | |
| Mouse monoclonal anti-GFP antibody | Roche Diagnostics | Cat#11814460001; RRID: AB_390913 |
| Mouse monoclonal anti-Myc antibody | Roche Diagnostics | Cat#11667149001; RRID: AB_390912 |
| Mouse monoclonal anti-HA antibody | Roche Diagnostics | Cat#11666606001; RRID: AB_514506 |
| Rat monoclonal anti-HA antibody | Roche Diagnostics | Cat#11867423001; RRID: AB_390918 |
| Mouse anti-Cytochrome c | Biolegend | Cat#612504; RRID: AB_2292697 |
| Cdc2 p34 antibody (PSTAIRE) | Santa Cruz Biotechnology | Cat#sc-53; RRID: AB_2074908 |
| Tri-methyl lysine motif rabbit mAb | Cell Signaling Technology | Cat#14680; RRID: AB_2798568 |
| HRP-linked anti-mouse IgG antibody | Amersham Biosciences | Cat#NA931 |
| HRP-linked anti-rabbit IgG antibody | Amersham Biosciences | Cat#NA934 |
| HRP-linked anti-rat IgG antibody | Cell Signaling Technology | Cat#7077S |
| EZview red anti-c-Myc affinity gel | Sigma-Aldrich | Cat#E6654 |
| Myc-Trap agarose | ChromoTek | Cat#yta-100 |
| Bacterial and virus strains | | |
| *E. coli* XL1-Blue competent cells | Agilent technologies | Cat#200228 |
| *E. coli* DH5α competent cells | Thermo Scientific | Cat#18263012 |
| Chemicals, peptides, and recombinant proteins | | |
| Sodium chloride | Sigma-Aldrich | Cat#746398; CAS: 7647-14-5 |
| Ampicillin | Sigma-Aldrich | Cat#A9393; CAS: 69-53-4 |
| Doxycycline | Sigma-Aldrich | Cat#D9891; CAS: 24390-14-5 |
| Uridine | Sigma-Aldrich | Cat#U3750; CAS: 58-96-8 |
| L-arginine | Sigma-Aldrich | Cat#A1270000; CAS: 74-79-3 |
| L-histidine | Sigma-Aldrich | Cat#H0755000; CAS: 71-00-1 |
| 5-fluoroorotic acid | Sigma-Aldrich | Cat#F5013; CAS: 207291-81-4 |
| Tween 20 | Sigma-Aldrich | Cat#P9416; CAS: 9005-64-5 |
| N-acetyl-glucosamine | Sigma-Aldrich | Cat#1010022; CAS: 7512-17-6 |
| Citric acid monohydrate | Sigma-Aldrich | Cat#C1909; CAS: 5949-29-1 |
| Potassium acetate | Sigma-Aldrich | Cat#P1190; CAS: 127-08-2 |
| Bovine serum albumin (BSA) | Sigma-Aldrich | Cat#A7906; CAS: 9048-46-8 |
| NP-40 | Sigma-Aldrich | Cat#492016; CAS: 9016-45-9 |
| Dithiothreitol (DTT) | Sigma-Aldrich | Cat#D0632; CAS: 3483-12-3 |
| Trichloroacetic acid (TCA) | Sigma-Aldrich | Cat#T6399; CAS: 76-03-9 |
| Bromophenol blue | Sigma-Aldrich | Cat#B0126; CAS: 115-39-9 |
| Methanol | Sigma-Aldrich | Cat#322415; CAS: 67-56-1 |
| Ethanol | Sigma-Aldrich | Cat#193511; CAS: 64-17-5 |
| Neutral buffered formalin | Sigma-Aldrich | Cat#HT501128 |
| Acid-washed glass beads | Sigma-Aldrich | Cat#G8772 |
| c-Myc peptide | Sigma-Aldrich | Cat#M2435 |
| LB broth (Miller) | Sigma-Aldrich | Cat#L3522 |
| Agar | Becton Dickinson | Cat#214010 |
| Yeast extract | Becton Dickinson | Cat#212750 |
| Yeast nitrogen base w/o amino acids (YNB) | Becton Dickinson | Cat#233520 |
| Yeast carbon base (YCB) | Becton Dickinson | Cat#239110 |
| Peptone | Gibco | Cat#211677 |

(*Continued on next page*)

*Continued*

| REAGENT or RESOURCE | SOURCE | IDENTIFIER |
|---|---|---|
| Tryptone | Gibco | Cat#211705 |
| D-Glucose | 1st Base | Cat#BIO1101 |
| Agarose | 1st Base | Cat#BIO1000 |
| Glycine | 1st Base | Cat#BIO2085 |
| Tris | 1st Base | Cat#BIO1400 |
| Tris HCl | 1st Base | Cat#BIO1500 |
| Potassium chloride | 1st Base | Cat#BIO1200 |
| Sodium Dodecyl Sulfate (SDS) | 1st Base | Cat#BIO2050 |
| 50X Tris-Acetate-EDTA (TAE) buffer | 1st Base | Cat#BUF300050X4L |
| 10X Phosphate Buffered Saline (PBS) | 1st Base | Cat#BUF204010X4L |
| Glycerol | Invitrogen | Cat#15514011 |
| Trizol | Invitrogen | Cat#15596018 |
| Nourseothricin | Jena Biosciences | Cat#AB102XL |
| KOD DNA polymerase | Merck | Cat#71085 |
| DreamTaq DNA polymerase | Thermo Scientific | Cat#EP1701 |
| MitoTraker red FM | Thermo Scientific | Cat#M22425 |
| Restore western blot stripping buffer | Thermo Scientific | Cat#21059 |
| Phusion DNA polymerase | New England Biolabs | Cat#M0530L |
| RNase free DNase I | New England Biolabs | Cat#M0303L |
| Protease inhibitor cocktail | Nacalai Tesque | Cat#0408011 |
| One-Step blue protein gel stain | Biotium | Cat#21003 |
| Critical commercial assays | | |
| GEL/PCR purification mini kit | Favorgen Biotech Corp | Cat#FAGCK001 |
| Plasmid DNA extraction mini kit | Favorgen Biotech Corp | Cat#FAPDE100 |
| Quickchange multi site-directed mutagenesis kit | Agilent technologies | Cat#200514 |
| Fast yeast transformation kit | G-Biosciences | Cat#GZ-1 |
| West pico chemiluminescent substrate | Thermo Scientific | Cat#34080 |
| MasterPure yeast DNA purification kit | Epicentre | Cat#MPY80200 |
| RNeasy mini kit | Qiagen | Cat#74104 |
| TruSeq RNA Library Prep Kit | Illumina | Cat#RS-122-2001/2 |
| iScript reverse transcription supermix | Bio-Rad | Cat#1708841 |
| iScript universal SYBR green supermix | Bio-Rad | Cat#1725121 |
| Double-stranded cDNA synthesis kit | Invitrogen | Cat#11917020 |
| Yeast mitochondria isolation kit | Sigma-Aldrich | Cat#MITOISO3 |
| PepTag non-radioactive cAMP dependent protein kinase assay kit | Promega | Cat#V5340 |
| ADP-Glo kinase assay kit | Promega | Cat#V6930 |
| Deposited data | | |
| Raw and analyzed RNA-Seq data | This paper | GEO: GSE243813 |
| Experimental models: Organisms/strains | | |
| *Candida albicans* strains; See Table S1 | This paper | N/A |
| Mouse: BALB/c | Jackson Laboratories | Cat#000651; RRID: IMSR_JAX:000651 |
| Oligonucleotides | | |
| ACT1-QF: CGATAACGGTTCTGG TATGTGTAAA | This paper | N/A |
| ACT1-QR: TCTTGGTCTACCAACAAGAGATGGG | This paper | N/A |
| ALS3-QF: CTGGACCACCAGGA ACACT | This paper | N/A |
| ALS3-QR: ACCTGGAGGAGCAGTGAAAG | This paper | N/A |
| ECE1-QF: GTCGTCAGATTGCCAGAAATTG | This paper | N/A |

(*Continued on next page*)

*Continued*

| REAGENT or RESOURCE | SOURCE | IDENTIFIER |
|---|---|---|
| ECE1-QR: CTTGGCATTTTCGATGGATTGT | This paper | N/A |
| HWP1-QF: GCTGGCTCAAGTGGTGCTAT | This paper | N/A |
| HWP1-QR: GGTTGCATGAGTGGAACTGA | This paper | N/A |
| NRG1-QF: CCCCATCCTTCCCAAGTACC | This paper | N/A |
| NRG1-QR: TGGGTCTTTGCTTTGGGTGT | This paper | N/A |
| UME6-QF: TCATTCTGCTGATTTGGTCAT | This paper | N/A |
| UME6-QR: TTGCAGCAGCACTAACACTG | This paper | N/A |
| RDN18-QF: GGACCCAGCCGAGCCTT | This paper | N/A |
| RDN18-QR: AAGTAAAAGTCCTGGTTCGCCA | This paper | N/A |
| **Recombinant DNA** | | |
| Plasmid: all plasmid constructs used in this study are listed in Table S2 | This paper | N/A |
| **Software and algorithms** | | |
| SeqPrep | GitHub | https://github.com/jstjohn/SeqPrep |
| Sickle | GitHub | https://github.com/najoshi/sickle |
| STAR | GitHub | https://github.com/alexdobin/STAR |
| FeatureCounts | Subread | https://subread.sourceforge.net/ |
| edgeR | Bioconductor | https://bioconductor.org/packages/release/bioc/html/edgeR.html |
| ImageJ | NIH | https://ImageJ.nih.gov/ij |
| Sequest HT | Thermo Scientific | https://www.thermofisher.com |
| Prism 9 | GraphPad | https://www.graphpad.com |
| CellQuest Pro | BD Biosciences | https://www.bdbiosciences.com |
| Motic Image Plus v3.0 | Motic | https://www.motic.com |
| MetaMorph v7.0 | Molecular Devices | https://www.moleculardevices.com |
| **Other** | | |
| FACSCalibur Flow Cytometer | BD Biosciences | https://www.bdbiosciences.com |
| NanoDrop 1000 Spectrophotometer | Thermo Scientific | https://www.thermofisher.com |
| CFX96 Touch Real-Time PCR qPCR system | Bio-Rad | https://www.bio-rad.com |
| 2100 Bioanalyser | Agilent | https://www.agilent.com |
| HiSeq X Ten System | Illumina | https://www.illumina.com |
| NovaSeq 6000 System | Illumina | https://www.illumina.com |
| MicroSmash MS-100 | Tomy Medico | https://www.digital-biology.co.jp |
| Infinite 200 Pro microplate reader | Tecan | https://www.tecan.com |
| LTQ-Orbitrap Velos Pro ETD | Thermo Scientific | https://www.thermofisher.com |
| LEITZ DMRB Microscope | Leica | https://www2.leicabiosystems.com |
| Moticam 10+ Camera | Motic | https://www.motic.com |
| Axiovert 200M Microscope | Zeiss | https://www.zeiss.com |
| CoolSnap HQ2 Camera | Photometrics | https://www.photometrics.com |

## RESOURCE AVAILABILITY

### Lead contact

Further information and requests for resources and reagents should be directed to and will be fulfilled by the lead contact, Yue Wang (wang_yue@idlabs.a-star.edu.sg).

### Materials availability

Strains and plasmids generated in this study are available upon request.

### Data and code availability

- Raw RNA-Seq reads and analyzed data generated in this study have been deposited in the Gene Expression Omnibus (GEO) database and are publicly available as of the date of publication. Accession numbers are listed in the key resources table. All other data reported in this paper will be shared by the lead author upon request.
- This paper does not report original code.
- Any additional information required to reanalyze the data reported in this work paper is available from the lead contact upon request.

## EXPERIMENTAL MODEL AND STUDY PARTICIPANT DETAILS

### Bacteria strains

*E.coli* competent cells XL1-blue and DH5α were purchased from commercial companies. They were used as the host strains for recombinant plasmids and cultured in LB broth (0.5% yeast extract, 1% tryptone, and 0.5% NaCl, pH 7.0) supplemented with 100 μg/mL ampicillin.

### *C. albicans* strains

*C. albicans* strains used in this study (Table S1) were derived from the clinic isolate SC5314. All haploid strains were verified for ploidy by flow cytometry analysis according to the published protocol.[56] *C. albicans* cells were routinely grown at 30°C in YPD (2% yeast extract, 1% peptone, and 2% glucose) or GMM (glucose minimal medium: 6.79 g/L yeast nitrogen base without amino acids and 2% glucose) supplemented with appropriate amino acids and other compounds (80 μg/mL uridine, 40 μg/mL arginine, 40 μg/mL histidine, and 1 mg/mL 5-fluoroorotic acid) when necessary. For the nonfermentable carbon source medium, glycerol was used to replace glucose. For media containing physiologically relevant carbon sources, the glucose in GMM was replaced with N-acetylglucosamine (GlcNAc), citric acid monohydrate (citrate), or potassium acetate, respectively. YCB-BSA medium contained 1.17% yeast carbon base, 0.5% bovine serum albumin, and 2% glucose with pH 4.0. Solid medium plates were prepared by adding agar to 2%. Serum plates contained 10% fetal bovine serum (FBS) and 2% agar. For hyphal induction, overnight yeast culture was diluted 1:20 into fresh medium containing 10% FBS and incubated at 37°C for durations as required. All gene deletion strains were verified by colony PCR as described,[56] and looping out of *URA3* or *SAT1* via FLP-mediated excision followed previous protocols.[74]

### Mouse lines

BALB/c mice were purchased from Jackson Laboratories (strain #000651; IMSR_JAX:000651) and bred in-house in a specific-pathogen-free animal facility on a 12:12 light-dark cycle. All animal experiments were conducted according to the rules and guidelines of the Agri-Food and Veterinary Authority and the National Advisory Committee for Laboratory Animal Research, Singapore. The experiments were approved by the Institutional Animal Care and Use Committee of the Biological Resource Center, Singapore (IACUC protocol #151010).

## METHOD DETAILS

### DNA manipulation and transformation

Recombinant DNA manipulations were performed according to standard methods. Site-directed mutagenesis followed the manual of the Quikchange multi-site-directed mutagenesis kit (Agilent). Transformation of *C. albicans* with plasmids containing prototrophic markers (including the *URA3* flipper, *UFP*) was performed using the Fast Yeast Transformation Kit (G-Biosciences). The electroporation method[56] was used to transform *C. albicans* with plasmids containing *SAT1* or *SAT1* flipper (*SFP*) as the selectable marker, and transformants were selected on YPD plates containing 200 μg/mL nourseothricin (Jena Biosciences).

### Transposon-mediated insertional haploid mutant library

To generate a transposon-mediated insertional haploid mutant library, the host strain YW02[37] was inoculated into 5 mL YPD medium containing 50 μg/mL doxycycline and cultured at 30°C overnight to induce the expression of *piggyBac* transposase. Cells were collected and washed twice with 25 mL GMM. Cells were then resuspended into 50 mL GMM and cultured at 30°C overnight to produce a collection of haploid transposon-insertional mutants. The quality of the mutant library was verified according to published procedures.[37] The library culture was then aliquoted and stored at −80°C for future use. To reveal the identity of genes mutated by transposon in isolated mutants, genomic DNA was extracted from each mutant and subjected to inverse PCR and DNA sequencing as described.[37]

### RNA extraction, cDNA preparation, and qRT-PCR

To compare gene expression levels, three biological replicates for each experiment were prepared, and total RNA was extracted with the RNeasy Mini Kit (Qiagen) according to manufacturer's instructions, followed by RNase-free DNase I (New England Biolabs) treatment to remove genomic DNA contamination. The total RNA was quantified before cDNA synthesis using NanoDrop 1000

spectrophotometer (Thermo Scientific). The iScript Reverse Transcription Supermix (Bio-Rad) was used to prepare cDNA. qPCR was set up in triplicates for each sample using the iTaq Universal SYBR Green Supermix (Bio-Rad) and performed on the CFX96 Touch Real-Time PCR detection system (Bio-Rad). The following thermal profile was used: 95°C for 30 s (initial denaturation), 40 cycles of 95°C for 5 s, and 60°C for 30 s (denaturation and annealing/extension). The specific primers used are listed in the Key Resources Table. Data analysis was performed according to the instrument-specific instructions, and gene expression levels were normalized against the housekeeping gene *ACT1*.

### RNA-seq and data analysis

Yeast cells were cultured in YPD at 30°C overnight and induced with 10% FBS for hyphal growth at 37°C for 1 and 2 h. The experiment was independently performed twice more, and samples were taken before hyphal induction and at 1 and 2 h after. Total RNA was extracted using the Trizol reagent according to the manufacturer's instructions (Invitrogen). Genomic DNA was removed using RNase-free DNase. RNA quality was determined by 2100 Bioanalyser (Agilent), and only high-quality RNA sample was used to construct the sequencing library. RNA-Seq transcriptome library was prepared from 1 ⌈g of total RNA using Illumina's TruSeq RNA sample preparation kit. Firstly, mRNA was isolated using oligo(dT) beads to select polyA mRNA and then fragmented with the fragmentation buffer. Secondly, double-stranded cDNA was synthesized using a SuperScript double-stranded cDNA synthesis kit (Invitrogen) with random hexamer primers (Illumina). Then the synthesized cDNA was subjected to end-repair, phosphorylation, and "A" base addition according to Illumina's library construction protocol. Libraries were size-selected for cDNA target fragments of 200–300 bp on 2% Low Range Ultra Agarose followed by PCR amplification using the Phusion DNA polymerase (New England Biolabs) for 15 PCR cycles. After quantification, the paired-end RNA-Seq sequencing library was sequenced using the Illumina HiSeq xten/NovaSeq 6000 sequencer. The Illumina platform converts the sequenced image signals into textual signals and stores them as raw data in the fastq format. Sequencing-related quality assessments were performed on the raw data for each sample.

For data analysis, the raw paired-end reads were trimmed and quality-controlled using the SeqPrep (https://github.com/jstjohn/SeqPrep) and Sickle (https://github.com/najoshi/sickle) software with default parameters. The clean reads were mapped to *C. albicans* reference genome SC5314 (assembly ASM18296v3) using the STAR aligner (version 2.2.1). Mapped reads were summarized to the gene level with the featureCounts software (version 1.6.3). Gene differential analysis was done using the Bioconductor R package edgeR in R (version 3.6.2). The Benjamini-Hochberg method was used for multiple testing corrections on p values. Differentially expressed genes (DEGs) were selected according to $\log_2$FC > 0.5, p value < 0.05 and FDR <0.05.

### Protein extraction, IP, and WB

To prepare yeast lysates, cells were harvested into 2-mL screw-cap microcentrifuge tubes by brief centrifugation to obtain pellets with a volume of ~400 μL and resuspended in 400 μL of ice-cold yeast lysis buffer (50 mM Tris-HCl [pH7.4], 150 mM KCl, 1% NP-40) containing the protease inhibitor cocktail (Nacalai Tesque). After adding an equal volume of acid-washed glass beads (Sigma-Aldrich), cells were broken by 5 rounds of 60-s beating at 5000 rpm in a MicroSmash MS-100 beater (Tomy Medico) with 1 min of cooling on ice between rounds. The lysed cells were then centrifuged at 16,000 rpm for 15 min at 4°C, and supernatants were collected.

To perform IP, yeast lysate was incubated with 30 μL of EZview Red Anti-*c*-Myc Affinity Gel (Sigma-Aldrich) or 20 μL of Myc-Trap agarose (ChromoTek) at 4°C for 1 h. After brief centrifugation at 2000 rpm, the beads were washed 3 times by resuspension in 1 mL cold yeast lysis buffer followed by brief centrifugation. The washed beads were resuspended in 20 μL of 2× protein loading buffer (125 mM Tris-HCl [pH 6.8], 4% SDS, 20% glycerol, 200 mM dithiothreitol, 0.02% bromophenol blue). To detect the target protein without IP, 5 μL of total protein lysate was mixed with 5 μL of 2× protein loading buffer. Sample mixtures were boiled for 10 min and separated by 8–12% SDS-PAGE gel. Subsequently, proteins on the gel were transferred using the transfer buffer (25 mM Tris, 192 mM glycine, 0.1% SDS, 20% methanol) to a polyvinylidene difluoride (PVDF) membrane (Bio-Rad) for WB, or the gel was stained with Coomassie blue to visualize the protein bands for MS analysis.

For WB, the PVDF membrane was first incubated with 5% milk blocking solution (dissolved in phosphate-buffered saline containing 0.1% Tween 20, PBST) at RT for 1 h or at 4°C overnight. After a brief rinse with PBST, the membrane was incubated in PBST containing a diluted primary antibody (monoclonal Myc, GFP, HA antibodies from Roche, or rabbit polyclonal trimethylated-lysine antibody from Cell Signaling) at RT for 1 h, followed by 3 rounds of 5-min wash with PBST. The membrane was then incubated with PBST containing a diluted secondary antibody (HRP-linked anti-mouse IgG, anti-rat IgG, and anti-rabbit IgG antibodies). After 3 rounds of 5-min wash with PBST, the membrane was immersed in West Pico Chemiluminescent Substrate (Thermo Scientific) and exposed to X-ray film (Fuji). All the bound antibodies were removed by Restore Western Blot Stripping Buffer (Thermo Scientific) to re-probe the membrane with another primary antibody if needed. To detect the level of Cdc28, rabbit polyclonal PSTAIRE (Santa Cruz) and HRP-linked anti-rabbit IgG were used as the primary and secondary antibodies, respectively.

### Differential fractionation of yeast mitochondria and cytosol

The yeast mitochondria and cytosol were separated by using the Yeast Mitochondria Isolation Kit (Sigma-Aldrich) according to the manufacturer's protocol. Briefly, 20 $OD_{600}$ of log phase cells (GZY1559 and GZY1561) were harvested, washed, and incubated with lyticase to digest cell walls. The resulting spheroplasts were lysed and centrifuged at 600 × g for 10 min. The supernatants were collected and further centrifuged at 6,500 × g for 10 min. The pellets contained mainly mitochondria and were dissolved in 50 μL

of 1× protein loading buffer. The new supernatants contained cytoplasmic proteins, to which trichloroacetic acid (TCA) was added to the final concentration of 10%. The precipitated proteins were washed once with 10% TCA solution and dissolved in 25 μL of 0.1 M NaOH and 25 μL of 2× protein loading buffer. The dissolved proteins were separated by SDS-PAGE and subjected to WB with anti-Cytochrome c and αHA antibodies.

### Immunopurification and *in vitro* PKA kinase assay

To purify Myc-tagged proteins, yeast extracts were prepared from strains expressing tagged proteins and incubated with Myc-Trap beads (Chromotek) at 4°C for 2 h. After washing 5 times with the lysis buffer, the beads were incubated with Myc peptide solution (50 ⌠g/mL, Sigma-Aldrich) at RT for 1 h on a roller, followed by centrifugation (8000 rpm, 1 min) to collect the supernatant. Aliquots of the elution products were subjected to WB to detect the Myc-tagged proteins. The densities of protein bands were measured using the ImageJ software to determine the relative protein concentrations of Cyc1-Myc, Cyc1$^{K79A}$-Myc, Myc-Tpk2, and Myc-Tpk1.

To examine the effect of Cyc1 binding on PKA kinase activity, equal amounts of eluted Myc-Tpk2 or Myc-Tpk1 were mixed with the Myc peptide elution products (in a ratio of 1:10) from BWP17, *cyc1*Δ/Δ:Cyc1-Myc, *cyc1*Δ/Δ:Cyc1$^{K79A}$-Myc, and *ctm1*Δ/Δ:Cyc1-Myc, respectively, in a total volume of 13 ⌠L and incubated at RT for 30 min. Each mixture was then used as the kinase to set up *in vitro* kinase reaction according to the instruction of the PepTag Non-Radioactive cAMP-Dependent Protein Kinase Assay kit (Promega) with slight modifications. Briefly, 13 ⌠L of the kinase mixture or Myc peptide elution buffer (the kinase control) was mixed with 5 ⌠L of 5× PKA Reaction Buffer, 5 ⌠L of 5× PKA Activator Solution, 1 ⌠L of Peptide Protection Solution, and 1 ⌠L of Kemptide (2 mg/mL). The mixture was incubated at RT for 30 min. Next, the kinase activity was determined using the ADP-Glo kinase Assay kit (Promega). Each kinase reaction was first mixed with 25 ⌠L of ADP-Glo Reagent and incubated at RT for 40 min. To terminate the kinase reaction and deplete the remaining ATP, 50 ⌠L of Kinase Detection Reagent was added to convert ADP to ATP. The newly synthesized ATP is quantitated using a luciferase/luciferin reaction. Finally, each reaction was aliquoted into three wells (30 ⌠L per well) on a 96-well plate. The luminescence of each well was recorded using a Tecan Infinite 200 Pro Microplate Reader (DKSH, Switzerland) and quantified as relative light units (RLU). The experiments were performed in triplicate, and data from three independent kinase assays were collected for further analysis.

### Mass spectrometry (MS) analysis

For MS analysis, the immunopurified proteins were separated by SDS-PAGE and the protein gel was stained with One-Step Blue (Biotium) according to the manufacturer's protocol. The target protein bands were excised, washed, reduced, alkylated, trypsin-digested, acidified, and desalted before concentration by SpeedVac vacuum as detailed in a filter-aided sample preparation method.[75] Samples were analyzed by liquid chromatography-tandem mass spectrometry (LC-MS/MS). Briefly, LTQ-Orbitrap Velos Pro ETD Mass Spectrometer (Thermo Scientific) was used for analysis, and tandem MS data were analyzed with Sequest HT in Protein Discoverer 1.4 SP1 (Thermo Scientific). The yeast protein database from UniProtKB/Swiss-Prot was used for the database search. In the decoy database search, the target false detection rate was set as q-value = 0.01. Multiconsensus reports were generated from multiple LC-MS results for different samples with collision-induced dissociation and high-energy collision dissociation acquisition modes.

### Optical and fluorescent microscopy

Morphological examination of yeast and filamentous cells was performed using the LEITZ DMRB optical microscope (Leica) equipped with a Moticam 10+ camera. Images were acquired using the Motic Image Plus 3.0 software. For mitochondria staining, strains expressing GFP-tagged Cyc1 or Cyc1$^{K79A}$ were cultured in GMM medium to mid-log phase at 30°C. Cells were collected and incubated with MitoTraker Red FM (Thermo Scientific) to stain mitochondria according to the instructions from the manufacturer. The stained cells were harvested, washed, and examined using the Axiovert 200M microscope (Zeiss) equipped with a CoolSnap HQ2 digital camera. Images were acquired and processed with the MetaMorph 7.0 software.

### Growth curve measurement

To determine the growth of *C. albicans* strains in different media, the strains were cultured at 30°C overnight and then diluted to an $OD_{600}$ of 0.1 in respective media. Each diluted culture was then aliquoted to 3 wells (200 μL/well) of a 96-well plate. Growth was recorded by measuring $OD_{600}$ in a microplate reader (Infinite M200 Pro, TECAN) at 37°C. Measurements were performed at 1-h intervals for not more than 72 h. Each measurement was performed with three independent biological replicates, and the results were shown as the mean ± SD. The media used in the experiments were YPD, GMM, YCB-BSA, 2% GlcNAc, 2% acetate, and 2% citrate.

### Virulence analysis

BALB/c mice between 8 and 10 weeks old were used for animal experiments. *C. albicans* strains were grown overnight in YPD medium at 30°C and harvested by centrifugation. Cells were washed twice with PBS and resuspended in PBS at the required density. For the systemic infection, each mouse was inoculated via the tail vein with 200 μL of a suspension containing either 8 x $10^5$ (high infectious dose) or 2 x $10^4$ (low infectious dose) C. albicans cells in PBS. Two infected mice from each group were sacrificed 48 h after inoculation, and the rest 8 mice were monitored for survival for up to 15 or 23 days. GraphPad Prism 9 was used to analyzed

survival and shown as Kaplan-Meyer curves. Survival curves were compared using the Log rank (Mantel-Cox) test and p values are shown in the graph.

### Histopathology and CFU counting

Mice were euthanized at 48 h post-infection to harvest kidneys. The kidneys were fixed with 10% (v/v) neutral buffered formalin. After dehydration with ethanol, kidneys were embedded in paraffin and cut into 5-μm longitudinal sections. Deparaffinized sections were mounted onto glass slides and stained with periodic acid-Schiff (PAS) reagent followed by hematoxylin counterstaining.

For colony-forming units (CFUs) analysis, the harvested organs (kidney, brain, liver, and spleen) were homogenized in PBS, serially diluted, and plated on YPD plates containing 100 μg/mL of ampicillin. The plates were incubated at 30°C for 24 to 48 h, and CFUs were counted and expressed as CFU per gram.

### Fungal burden measurement by qPCR

Mice infected with various *C. albicans* strains (3 per strain) were euthanized 48 h post-infection to harvest kidneys. After weighing, the kidneys were homogenized in water, and the homogenates were filtered through a cell strainer (70 μm Nylon, BD Falcon), followed by centrifugation at 4000 x g for 5 min. Genomic DNA was extracted from the pellet using the MasterPure Yeast DNA Purification Kit (Epicentre) following manufacturer's instructions and dissolved in 50 μL water. For qPCR, the following primers for *C. albicans* rRNA gene *RDN18* were used: the sense primer, 5'-GGACCCAGCCGAGCCTT-3', and the antisense primer, 5'-AAGTAAAA GTCCTGGTTCGCCA-3'. The extracted DNA was diluted 30-fold and 4 μL of the diluted DNA was used as the template in a 20 μL reaction system. qPCR was set up in triplicates for each sample using the iTaq Universal SYBR Green Supermix (Bio-Rad) and performed on the CFX96 Touch Real-Time PCR detection system (Bio-Rad). The following conditions were used for product amplification: 95°C for 15min, 40 cycles of each 95°C for 15 s, 59°C for 15 s and 72°C for 15 s. The resulting cycle threshold (Ct) values were used to calculate the corresponding fungal cell numbers. Fungal burden was represented by the cell number per gram of mouse kidney. To correlate Ct value with cell number, genomic DNA was extracted from different amounts of *C. albicans* cells (ranging from $1x10^5$ to $5x10^7$) to generate a standard curve between DNA amount and cell numbers. Next, different amounts of genomic DNA were used as templates for qPCR to produce another standard curve correlating the DNA amount and the Ct value.

## QUANTIFICATION AND STATISTICAL ANALYSIS

For statistical analysis, three independent biological replicates for each condition were used. Data were analyzed using Excel (unless otherwise specified) and presented as means ± SD (standard deviation). The one-way or two-way student's *t*-test (stated in figure legends) was used to check for statistical significances. p values $\leq 0.05$ were considered significant, *p $\leq$ 0.05; **p $\leq$ 0.01; ***p $\leq$ 0.001. All data needed to evaluate the conclusions in the paper are present in the paper and/or the Supplementary Materials.